PNNL-10987
UC-~~810~~ 2000
Project Technical Information

Effect of Composition and Temperature on the Properties of High-Level Waste (HLW) Glass Melting Above 1200°C (DRAFT)

J. D. Vienna
P. R. Hrma
M. J. Schweiger
M. H. Langowski
P. E. Redgate
D. S. Kim
G. F. Peipel
D. E. Smith
C. Y. Chang
D. E. Rinehart
S. E. Palmer
H. Li

February 1996

Prepared for
the U.S. Department of Energy
under Contract DE-AC06-76RLO 1830

Pacific Northwest National Laboratory
Richland, Washington 99352

PNNL-10987
UC-810
Project Technical Information

Effect of Composition and Temperature on the Properties of High-Level Waste (HLW) Glasses Melting Above 1200°C (Draft)

J. D. Vienna
P. R. Hrma
M. J. Schweiger
M. H. Langowski
P. E. Redgate
D. S. Kim
G. F. Piepel
D. E. Smith
C. Y. Chang
D. E. Rinehart
S. E. Palmer
H. Li

February 1996

Prepared for
the U.S. Department of Energy
under Contract DE-AC06-76RLO 1830

Pacific Northwest National Laboratory
Richland, Washington 99352

DISCLAIMER

PACIFIC NORTHWEST NATIONAL LABORATORY
operated by
BATTELLE
for the
UNITED STATES DEPARTMENT OF ENERGY
under Contract DE-AC06-76RLO 1830

Printed in the United States of America

Available to DOE and DOE contractors from the Office of Scientific and Technical Information, P.O. Box 62, Oak Ridge, TN 37831; prices available from (615) 576-8401.

Available to the public from the National Technical Information Service, U.S. Department of Commerce, 5285 Port Royal Rd., Springfield, VA 22161

The document was printed on recycled paper.

Summary

Increasing the melting temperature of HLW glass allows an increase of waste loading (thus reducing product volume) and the production of more durable glasses at a faster melting rate. However, HLW glasses that melt at high temperatures differ in composition from glasses formulated for low temperature (~1150°C). Consequently, the composition of high-temperature glasses falls in a region previously not well tested or understood. This report represents a preliminary study of property/composition relationships of high-temperature Hanford HLW glasses using a one-component-at-a-time change approach.

A test matrix has been designed to explore a composition region expected for high-temperature high-waste loading HLW glasses to be produced at Hanford. This matrix was designed by varying several key components (SiO_2, B_2O_3, Na_2O, Li_2O, Fe_2O_3, Al_2O_3, ZrO_2, Bi_2O_3, P_2O_5, UO_2, TiO_2, Cr_2O_3, and Others) starting from a glass based on a Hanford HLW all-blend waste. Glasses were fabricated and tested for viscosity, glass transition temperature, electrical conductivity, crystallinity, liquidus temperature, and PCT release. The effect of individual components on glass properties was assessed using first- and second-order empirical models. The first-order component effects were compared with those from low-temperature HLW glasses.

Table of Contents

1.0 Introduction

High-Level Waste (HLW) at Hanford will be converted into a vitrified form for disposal in a geological repository. Nearly 230,000 m^3 (61 million gallons) of nuclear waste are stored at Hanford in 28 double shell tanks (DSTs) and 149 single shell tanks (SSTs). These wastes will be separated into HLW and Low-Level Waste (LLW) and vitrified. Current Tank Waste Remediation System (TWRS) flowsheets indicate that wastes from DST's and SST's will first be blended, pretreated by sludge washing, and separated into HLW and LLW fractions for vitrification.

To formulate glasses for HLW vitrification, the Composition Variation Study (CVS) was undertaken. This study was undertaken to measure and model glass properties as a function of composition. This effort initially focused on glasses expected to be melted at 1150°C containing 25 to 28 wt% of pretreated Hanford Double Shell Tank (DST) Waste, in particular, Neutralized Current Acid Waste (NCAW). The study results are discussed in detail by Hrma and Piepel et al. (1994) and are referred to extensively here.

Characterization of tank wastes is still in progress and pretreatment processes are under development. The chemical compositions of the pre-treated wastes will likely differ considerably from current estimates. Uncertainty in waste composition exists from tank-to-tank variations, tank composition characterization uncertainty, and undecided pretreatment and blending processes, and process control considerations. This uncertainty can be addressed by developing models that can be used for glass formulation over the range of HLW compositions expected to be vitrified at Hanford. Such composition variation (composition envelope) studies constitute a part of the overall glass formulation strategy for addressing HLW vitrification needs. The strategy also involves performing more detailed studies of selected waste composition estimates to determine solubility, crystallinity, or other limits on waste loading. Knowledge of such limits and the ability to formulate glasses over composition regions appropriate for Hanford site wastes are needed to support waste blending and pretreatment decisions. Once such decisions are made and waste types to be processed by a Hanford HLW vitrification plant are selected, glass formulation efforts can then focus on developing robust glass compositions for these waste types.

The fraction of waste oxides or waste loading (WL) in Hanford waste glass will ultimately influence the cleanup cost. Increasing WL should reduce the time to process waste, which will decrease the cost of materials, equipment, and labor. Immobilized waste volume and repository space will also be reduced by increased WL. It is estimated that waste disposal in a repository will make up a large fraction of nuclear waste cleanup costs (Merrill and Chapman, 1994). Maximum WL must be compatible with processing and product acceptability requirements imposed on glass. Waste loading is limited by processing requirements through melting and liquidus temperatures (T_M and T_L, respectively) or melt segregation. Product quality limits waste loading through a restriction on product durability.

Experience has shown that the restriction $T_L \leq T_M$-100°C, generally accepted as the T_L limit for continuous melters, will constrain the WL for a majority of Hanford high level wastes (see Lambert and Kim 1994 and Hrma and Vienna 1995). In this case, the maximum waste loading will be determined as the point with the highest waste loading while maintaining a separation of 100°C between the curves of T_L and T_M. These temperatures can be measured or predicted using thermodynamic and property/composition models, respectively. Although T_L tends to increase with WL, the difference between T_L and T_M decreases with waste loading for several Hanford waste composition estimates. If T_M is further restricted by low temperature processing technology, then WL is also limited. Additional processing constraints may further limit WL. Some commonly encountered constraints are discussed elsewhere, including: molten salt

segregation (Li et al. 1995), immiscible phase separation (Peeler and Hrma 1994), and component solubility (Langowski et al. 1994, Li et al. 1995).

Higher melting temperature glasses are needed to increase WL in waste glass. In this regard property composition relationships must be studied in a different glass composition region than that used for lower temperature melting glasses. The four major differences between the composition region for low temperature glasses of the CVS and the high temperature glasses of the CVS are: 1) decreased boron concentration, 2) increased refractory concentration (i.e. Al, Fe, and Zr), 3) larger range of SiO_2 concentrations, and 4) different "Others" composition. These differences are shown in the composition summary table below. In addition to these four compositional changes, P_2O_5, Bi_2O_3, and UO_2 have been added to the high-temperature phase of the study.

Table I. Composition range of CVS and HTM glasses in mass fractions.

Oxide	CVS Range		HTM Range	
	Lower Limit	Upper Limit	Lower Limit	Upper Limit
SiO_2	0.420	0.570	0.370	0.600
B_2O_3	0.050	0.200	0.000	0.084
Na_2O	0.050	0.200	0.050	0.226
Li_2O	0.010	0.070	0.000	0.072
CaO	0.000	0.100	*	*
MgO	0.000	0.080	*	*
Fe_2O_3	0.005	0.150	0.000	0.150
Al_2O_3	0.000	0.170	0.000	0.250
ZrO_2	0.000	0.130	0.000	0.160
Others	0.010	0.100	0.080	0.200
Bi_2O_3			0.007	0.164
P_2O_5			0.007	0.090
UO_2			0.000	0.148

Additional CVS composition constraints: Components	Upper	HTM Range
Al2O3 / SiO2	0.33	0.00 - 0.59
MgO + CaO	0.10	0.01 - 0.02
Al2O3 + ZrO2	0.16	0.05 - 0.28
Al2O3 + Fe2O3 + ZrO2 + Others	0.24	0.25 - 0.45

* indicates components that are present only in waste and not independently altered

The objective of this report is to describe the effects of composition on the following waste glass properties and characteristics: melting temperature (T_M), viscosity (η)-temperature relationship, glass transition temperature (T_g), electrical conductivity (ε), liquidus temperature (T_L), canister centerline cooling (CCC) crystallinity, and product consistency test (PCT) releases (r_i where i indicates the i-th component release) from quenched and CCC glasses.

The effect of composition on glass properties can be expressed by means of first-order model coefficients, which correspond to partial specific properties (Hrma and Robertus 1993). Alternatively, component effects can be expressed in terms of the change in the property if a

component is added to the mixture (glass). The effects can be described and used in several different ways. The effect of a single component can be taken as the slope at the zero addition point of a property versus component addition curve. The slope can then be converted into a first-order model coefficient which is used to predict property values from glass composition. These models are used in several tasks including glass formulation, evaluation of blending and pretreatment scenarios, selection of melter technologies, HLW plant operation, and waste form qualification.

The work covered in this report is discussed in the test plan (Langowski et al. 1994). The completion of this report satisfies milestones PVTD-C95-02.01E and PVTD-C95-02.01J. The report is organized by property, then further broken down to components.

2.0 Mathematical Modelling

Currently, acceptable physical or theoretical models relating glass properties to composition do not exist due to the complexity of glass chemistry. PNL therefore bases property modelling on theoretically justifiable mixture model forms with empirically fit coefficients (Hrma and Piepel et al. 1994). This method yields good property prediction capability for a given composition range where no discontinuities exist in properties. However, models must be fit to experimental data in the composition range of interest. Extrapolation outside of that range will dramatically increase the uncertainty of property predictions made with such models.

If glass is taken as a mixture of components, a mixture property (π) depends on primary thermodynamic variables including temperature (T), pressure (P), and composition vector (g). Since P is constant for glass melting operations, $\pi = f(T, g)$. Viscosity and electrical conductivity data were generated as a function of temperature in this study. The dependence of these properties on temperature follow the Vogel-Fulcher-Tammann (VFT) relationship:

$$\ln(\pi) = A(g) + \frac{B(g)}{T - T_0(g)} \tag{1}$$

where, A, B, and T_0 are temperature independent material constants. Equation (1) can be reduced to a linear relationship for narrow temperature intervals to form the Arrhenius equation:

$$\ln(\pi) = E(g) + \frac{F(g)}{T} \tag{2}$$

where E and F are temperature independent material constants. The constants A, B, T_0, E, and F can then be modeled as functions of composition.

The empirical model form is that of a simple first- or second-order mixture model with coefficients for major oxide components:

$$p = \sum_{i=1}^{n} a_i g_i + \sum_{i=1}^{n-1} \sum_{j>i}^{n} b_{ij} g_i g_j \tag{3}$$

where p is the transformed property (such as $\ln r_{Na}$), g_i is the i-th component mass fraction, and a_i and b_{ij} are the first- and second-order model coefficients. A second-order model has a limited number of nonzero b_{ij}'s, whereas all b_{ij}'s are zero in the first-order model. Component effects are given by the slope of p vs. component change curve at a given composition point. This slope

can be calculated from Equation (3) for a first-order model:

$$\frac{\partial p}{\partial g_\alpha} = \frac{a_\alpha - p}{1 - g_\alpha} \tag{4}$$

where, $\partial p/\partial g_\alpha$ is the effect of adding (or subtracting) the α-th component on p. The effect of replacing component β by component α can also be expressed simply for the first-order model as:

$$\frac{\partial p}{\partial g_\alpha} = a_\alpha - a_\beta. \tag{5}$$

These relationships will be further discussed in this report. A table of properties and their associated coefficients are listed in the summary.

3.0 Experimental Approach

A composition envelope approach has been used to characterize the property / composition relationships for Hanford waste glasses. A one-component-at-a-time change study was chosen for the first phase of the higher glass melting temperature CVS because of the large composition range, non-linear component effects, and the number of components which may vary in the waste glass. This study is the first of two steps described in detail in the test plans for each stage (Langowski et al. 1994 and Piepel et al. 1995). The baseline glass (CVS3-1) was formulated from 50 wt% of Hanford waste blend simulant and additives to allow melting at 1350°C.

The test matrix in Table II includes glasses varied one-component-at-a-time with the remaining components in the same relative proportion as in the baseline glass (CVS3-1). The components varied are SiO_2 (2 to 5), B_2O_3 (6 and 7), Na_2O (8 and 9), Li_2O (10 to 12), Fe_2O_3 (13 to 15 and 27), Al_2O_3 (16 to 19), ZrO_2 (20 to 23), Others (24 and 25), Bi_2O_3 (28 to 31), UO_2 (32 to 36), and P_2O_5 (37 to 40). As most glasses contain Nd_2O_3 as a substitute for UO_2, the baseline glass for UO_2 change is CVS3-32 with Nd replaced by U on a nearly one-to-one molar basis.

Additional studies that have varied components one-at-a-time from other baseline glass compositions include:

- HTB651 — P_2O_5, TiO_2, and Cr_2O_3 (Li et al. 1995),
- PFP — P_2O_5 (Li et al. 1995),
- HW39-4 — SiO_2, B_2O_3, Na_2O, Li_2O, CaO, MgO, and Al_2O_3 (Hrma, Piepel, et al. 1994), and
- WV205 — SiO_2, Na_2O, Li_2O, Al_2O_3, Fe_2O_3, ZrO_2, TiO_2, and Cr_2O_3 (Feng 1989).

Table II. HTM test matrix in mass fractions (Langowski et al. 1994).

Glass #	SiO_2	B_2O_3	Na_2O	Li_2O	Fe_2O_3	Al_2O_3	ZrO_2	Bi_2O_3	P_2O_5	UO_2	Others
CVS3-1	**0.5333**	**0.0005**	**0.1234**	**0.0286**	**0.0680**	**0.0487**	**0.0438**	**0.0137**	**0.0079**	**0.0000**	**0.1321**
CVS3-2	**0.6000**	0.0004	0.1057	0.0245	0.0583	0.0417	0.0375	0.0118	0.0068	0.0000	0.1133
CVS3-3	**0.4500**	0.0005	0.1454	0.0337	0.0801	0.0574	0.0516	0.0162	0.0094	0.0000	0.1557
CVS3-4	**0.4000**	0.0006	0.1586	0.0367	0.0874	0.0626	0.0563	0.0176	0.0102	0.0000	0.1700
CVS3-5	**0.3700**	0.0006	0.1665	0.0386	0.0918	0.0657	0.0591	0.0185	0.0107	0.0000	0.1785
CVS3-6	0.4889	**0.0837**	0.1131	0.0262	0.0623	0.0446	0.0401	0.0126	0.0073	0.0000	0.1212
CVS3-7	0.5122	**0.0400**	0.1185	0.0274	0.0653	0.0468	0.0420	0.0132	0.0076	0.0000	0.1270
CVS3-8	0.4710	0.0004	**0.2258**	0.0252	0.0600	0.0430	0.0387	0.0121	0.0070	0.0000	0.1168
CVS3-9	0.5779	0.0005	**0.0500**	0.0309	0.0737	0.0527	0.0474	0.0149	0.0086	0.0000	0.1434
CVS3-10	0.5097	0.0004	0.1179	**0.0716**	0.0650	0.0465	0.0418	0.0131	0.0076	0.0000	0.1264
CVS3-11	0.5215	0.0005	0.1206	**0.0500**	0.0665	0.0476	0.0428	0.0134	0.0078	0.0000	0.1293
CVS3-12	0.5490	0.0005	0.1270	**0.0000**	0.0700	0.0501	0.0451	0.0141	0.0082	0.0000	0.1360
CVS3-13	0.4864	0.0004	0.1125	0.0260	**0.1500**	0.0444	0.0399	0.0125	0.0072	0.0000	0.1207
CVS3-14	0.5093	0.0004	0.1178	0.0273	**0.1100**	0.0465	0.0418	0.0131	0.0076	0.0000	0.1262
CVS3-15	0.5722	0.0005	0.1324	0.0306	**0.0000**	0.0522	0.0470	0.0147	0.0085	0.0000	0.1419
CVS3-16	0.4204	0.0004	0.0972	0.0225	0.0536	**0.2500**	0.0345	0.0108	0.0063	0.0000	0.1043
CVS3-17	0.4597	0.0004	0.1063	0.0246	0.0586	**0.1800**	0.0377	0.0118	0.0068	0.0000	0.1141
CVS3-18	0.4877	0.0004	0.1128	0.0261	0.0622	**0.1300**	0.0400	0.0126	0.0073	0.0000	0.1209
CVS3-19	0.5606	0.0005	0.1297	0.0300	0.0715	**0.0000**	0.0460	0.0144	0.0084	0.0000	0.1389
CVS3-20	0.4685	0.0004	0.1084	0.0251	0.0597	0.0428	**0.1600**	0.0121	0.0070	0.0000	0.1160
CVS3-21	0.4908	0.0004	0.1135	0.0263	0.0626	0.0448	**0.1200**	0.0126	0.0073	0.0000	0.1217
CVS3-22	0.5131	0.0004	0.1187	0.0275	0.0654	0.0468	**0.0800**	0.0132	0.0076	0.0000	0.1273
CVS3-23	0.5577	0.0005	0.1290	0.0299	0.0711	0.0509	**0.0000**	0.0144	0.0083	0.0000	0.1382
CVS3-24	0.4966	0.0004	0.1149	0.0266	0.0633	0.0453	0.0408	0.0195	0.0113	0.0000	**0.1813**
CVS3-25	0.5742	0.0005	0.1328	0.0307	0.0732	0.0524	0.0471	0.0073	0.0042	0.0000	**0.0776**
CVS3-26	0.5328	0.1048	0.1129	0.0373	0.0733	0.0235	0.0392	0.0000	0.0010	0.0000	0.0752
CVS3-27	0.4864	0.0004	0.1125	0.0260	**0.1500**	0.0444	0.0399	0.0125	0.0072	0.0000	0.1207
CVS3-28	0.5170	0.0005	0.1196	0.0277	0.0659	0.0472	0.0424	**0.0437**	0.0077	0.0000	0.1283
CVS3-29	0.5062	0.0005	0.1171	0.0271	0.0645	0.0462	0.0416	**0.0637**	0.0075	0.0000	0.1256
CVS3-30	0.4792	0.0005	0.1109	0.0257	0.0611	0.0437	0.0393	**0.1137**	0.0071	0.0000	0.1188
CVS3-31	0.4522	0.0004	0.1046	0.0242	0.0576	0.0413	0.0371	**0.1637**	0.0067	0.0000	0.1122
CVS3-32	**0.5306**	**0.0004**	**0.1146**	**0.0287**	**0.0631**	**0.0452**	**0.0407**	**0.0127**	**0.0074**	**0.0900**	**0.0616**
CVS3-33	0.5644	0.0005	0.1219	0.0305	0.0672	0.0481	0.0432	0.0135	0.0078	**0.0320**	0.0690
CVS3-34	0.5475	0.0004	0.1182	0.0296	0.0652	0.0467	0.0420	0.0131	0.0076	**0.0610**	0.0652
CVS3-35	0.5136	0.0004	0.1109	0.0277	0.0611	0.0438	0.0394	0.0123	0.0071	**0.1190**	0.0583
CVS3-36	0.4966	0.0004	0.1072	0.0268	0.0591	0.0423	0.0381	0.0119	0.0069	**0.1480**	0.0550
CVS3-37	0.5214	0.0005	0.1206	0.0279	0.0665	0.0476	0.0428	0.0134	**0.0300**	0.0000	0.1293
CVS3-38	0.5107	0.0005	0.1181	0.0274	0.0651	0.0466	0.0419	0.0131	**0.0500**	0.0000	0.1266
CVS3-39	0.4999	0.0005	0.1156	0.0268	0.0637	0.0456	0.0410	0.0129	**0.0700**	0.0000	0.1240
CVS3-40	0.4892	0.0005	0.1132	0.0262	0.0624	0.0447	0.0402	0.0126	**0.0900**	0.0000	0.1210

The glasses in Table II were fabricated and tested according to standard test procedures in the Glass Development Laboratory at PNL (Hrma, Piepel, et al. 1994). The following properties and characteristics have been measured and summarized:

- transition temperature (dilatometric),
- viscosity (300°C interval near 5 Pa.s),
- electrical conductivity (same temperature interval as viscosity, 0.01 to 100 KHz),
- liquidus temperature,
- quenched and CCC crystallinity, and
- product consistency test (PCT) releases from quenched and CCC glasses.

4.0 Process Related Properties

The processing related properties of practical significance to waste vitrification are T_g, viscosity (η), electrical conductivity (ε), and T_L. A summary of these properties is given in Table III. The coefficients A, B, and T_0 were obtained by non-linear least squares fitting of the viscosity-temperature data. The second set of A, B, and T_0 values were fit using an additional data point ($\eta = 10^{11.3}$ Pa.s) at the glass transition temperature. The E and F coefficients were obtained by a linear regression fit of the Arrhenius Equation (2) to the viscosity and electrical conductivity data found in Sections 10.2 and 10.3, respectively. The results for glass melting temperature, viscosity, electrical conductivity, and glass transition temperature are discussed in the following subsections. First- and second-order models have been fitted statistically to this data and are presented in Section 6.0. The response of many process related properties to changing components are nonlinear as figures in this section show. In these cases, nonlinear (second-order) models, found in Table XI, may give better property predictions.

Table III. Processing related parameters (T_g, VFT A, B, and T_0 for viscosity, Arrhenius E and F for viscosity and electrical conductivity, and T_M).

Glass	Glass Name	Tg (°C)	Tm (°C)	Ln [Viscosity (Pa·s)]								Electrical Conductivity		
				VFT			VFT with Tg data pt.			Arrhenius		ln [ε (S/m)]		S/m @
				A	B (K)	To (K)	A	B (K)	To (K)	E	F (K)	E	F (K)	5 Pa·s
CVS3-1	Baseline	498.9	1366	-7.2	10073.0	492.1	-7.7	11082.0	443.0	-12.04	22335.1	8.6	-7739.1	48.92
CVS3-2	High Si	509.3	1500	-2.6	3388.7	979.1	-7.7	12630.0	407.9	-11.32	22774.9	8.8	-8783.1	47.08
CVS3-3	Med Si	484.3	1213	-8.2	9715.8	490.4	-8.6	10494.0	453.9	-13.61	22648.3	9.0	-7648.7	45.92
CVS3-4	Low Si	457.3	1155				-8.9	10550.0	428.7	-13.64	21802.3	9.1	-7455.4	47.79
CVS3-5	Very Low Si	449.1	1165							-39.99	59812.9	8.8	-6755.4	60.90
CVS3-6	High B (η = 2)	503.4	1237	-7.9	10857.0	366.6	-6.3	7660.8	539.5	-11.24	19441.9	8.6	-7874.1	29.76
CVS3-7	Med B	505.3	1301	-6.1	7680.2	577.2	-6.7	8913.9	506.3	-11.31	20355.7	8.5	-7593.9	37.64
CVS3-8	High Na (η = 2)	441.2	1182	-8.6	11477.0	332.8	-7.6	9367.2	435.6	-11.95	19755.5	8.4	-6065.9	71.82
CVS3-9	Low Na	538.4	1529	-3.4	4309.2	942.4	-7.8	12870.0	431.1	-11.53	23596.9	8.6	-9156.5	34.10
CVS3-10	High Li (η = 2)	457.4	1153	-6.5	6836.5	584.0	-7.9	9189.2	459.5	-12.91	20788.1	9.2	-7453.8	55.29
CVS3-11	Med Li	473.5	1257	-6.9	8702.9	501.4	-7.3	9470.3	462.1	-12.05	20895.7	8.6	-7154.8	52.46
CVS3-12	No Li	562.8	1557	-3.3	4247.6	977.9	-8.6	14211.0	425.0	-12.58	25798.1	7.9	-7548.9	42.10
CVS3-13	High Fe	493.3	1310				-8.1	11091.0	441.4	-12.45	22264.6	8.4	-7528.5	39.26
CVS3-14	Med Fe	504.5	1335	-8.2	11874.0	401.9	-7.6	10578.0	463.3	-12.19	22179.8	8.7	-7808.7	44.42
CVS3-15	No Fe	490.6	1419	-6.9	10081.0	508.2	-7.9	12227.0	403.0	-11.62	22350.5	8.1	-6949.4	53.46
CVS3-16	Very High Al	543.1	1516							-15.79	31140.1	8.2	-8098.3	39.36
CVS3-17	High Al	571.9	1506	-3.8	4518.2	948.9	-8.3	12905.0	468.5	-12.57	25176.8	7.9	-7220.1	46.82
CVS3-18	Med Al	532.0	1457	-4.2	5022.3	863.4	-8.1	12600.0	436.4	-12.20	23840.3	8.3	-7654.4	50.42
CVS3-19	No Al	484.3	1309	-6.2	7808.3	584.3	-7.5	10255.0	451.2	-11.66	20994.0	10.6	-10176.4	67.48
CVS3-20	High Zr	525.9	1456							-16.61	31494.5	9.2	-8801.9	59.08
CVS3-21	Med Zr	506.2	1376				-10.8	16360.0	335.6	-14.54	26635.5	9.6	-9227.2	52.52
CVS3-22	Low Zr	500.6	1366	-6.4	7887.1	655.4	-9.2	13503.0	390.4	-13.33	24483.5	8.4	-8021.9	34.07
CVS3-23	No Zr	477.4	1355	-6.1	8624.7	513.0	-6.6	9599.9	456.1	-10.23	19285.4	8.2	-6847.1	51.97
CVS3-24	High Others	510.9	1324	-10.6	17178.0	188.2	-7.8	10535.0	472.1	-12.46	22463.8	8.5	-7752.1	38.91
CVS3-25	Low Others	489.0	1411	-6.4	9108.6	547.0	-7.4	11443.0	420.2	-10.89	21058.0	9.5	-8766.2	76.67
CVS3-27	Replicate (#13)	491.0	1308				-8.0	10939.0	442.5	-12.30	22012.2	8.5	-7685.5	39.24
CVS3-28	Low Bi	475.0	1349	-5.3	6550.7	671.7	-7.8	11330.0	412.8	-11.73	21601.3	8.8	-8042.4	44.51
CVS3-29	Med Bi	472.0	1336	-5.7	7242.1	623.2	-7.7	11101.0	415.9	-11.62	21281.6	8.3	-7434.2	41.20
CVS3-30	High Bi	466.0	1299	-5.2	6062.3	677.0	-7.8	10863.0	418.0	-12.09	21496.7	8.7	-7958.5	37.73
CVS3-31	Very High Bi	469.5	1261	-6.1	7152.5	601.3	-8.0	10530.0	432.8	-12.85	22130.1	9.1	-8522.6	34.11
CVS3-32	High U		1388	-4.9	5810.8	762.6				-12.06	22652.7			
CVS3-33	Low U		1410	-4.0	4904.8	816.2				-11.70	22277.1			
CVS3-34	Med U	N/A	1410	-2.3	2504.3	1035.1	N/A			-12.32	23248.5	N/A		N/A
CVS3-35	Very High U		1381	-3.4	3717.8	917.3				-12.53	23315.2			
CVS3-36	X Very High U		1372	-1.6	1563.1	1154.7				-10.75	20346.7			
CVS3-37	Low P	470.5	1378	-6.3	8214.7	606.9	-8.4	12886.0	369.8	-11.86	22236.4	8.3	-7195.8	50.02
CVS3-38	Med P	474.0	1391	-6.4	8599.9	590.0	-8.5	13030.0	369.2	-11.90	22463.8	8.2	-7076.5	51.80
CVS3-39	High P	503.0	1408	-4.5	5383.3	795.1	-8.0	12128.0	419.9	-12.00	22833.0	8.1	-7206.9	43.70
CVS3-40	Very High P	516.0	1417	-5.8	7434.1	687.1	-8.2	12422.0	426.4	-12.19	23294.0	7.9	-6730.2	50.39

4.1 Melting Temperature

Since viscosity is a function of both temperature and composition, the effect of composition can be shown in three ways: 1) effects of components on viscosity at a set temperature, 2) effects of components on temperature at a fixed viscosity, and 3) component effects on the VFT parameters A, B, and T_0. This study has been designed to develop property data for glasses melting over a range of temperatures suitable for processing in a high-temperature melter. Hence, option one is not considered.

The effect of components on the T_M of the glass, where T_M is the temperature at a viscosity of 5 Pa·s, can be seen in Figure 1. Table IV shows the slopes of T_M versus component mass fractions (component effects). A first-order model has been fitted to the CVS T_M data (including

low and high temperature phases). The model coefficients (a_i from Equation (3)) are compared to those calculated from CVS3-1 measured effects using Equation (4) and are listed in Table V.

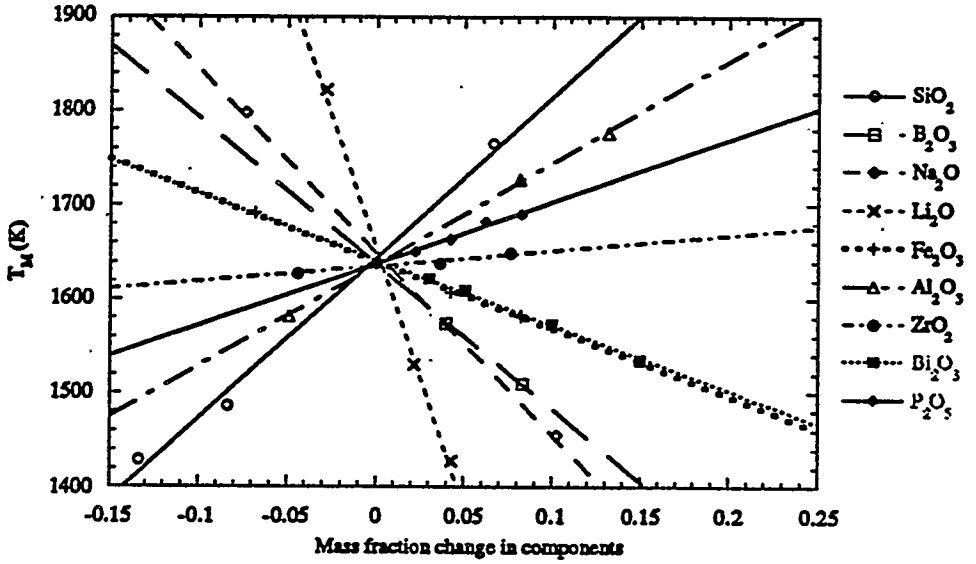

Figure 1. Effects of components on T_M for CVS3-1 baseline glass.

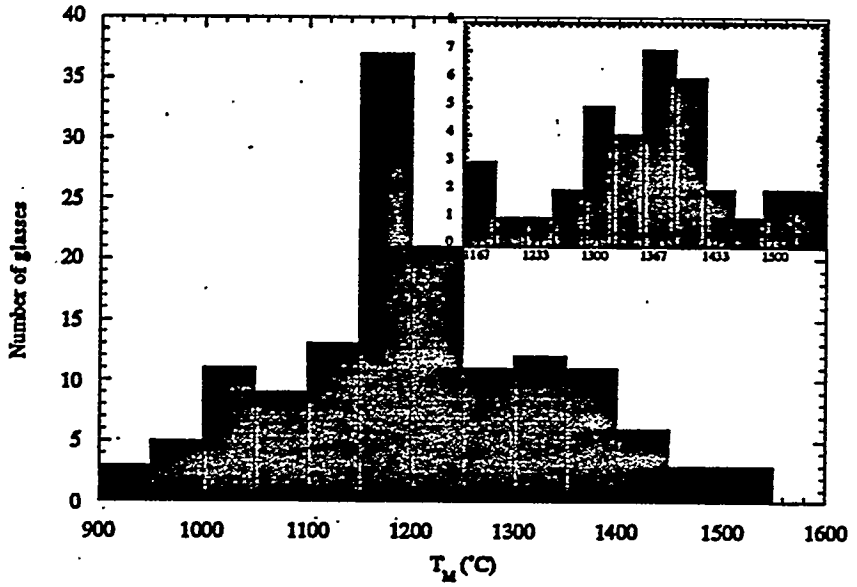

Figure 2. Histogram of measured T_M for CVS-I, -II, and -III glasses. CVS-III glasses are shown in the insert.

Figure 2 shows the histogram of melting temperatures for the combined CVS study, showing that a T_M range from 900 to 1540°C has been covered. The CVS- I and -II glasses alone range from 900 to 1450°C, although a majority of low-temperature glasses melt below 1250°C. A histogram

of T_M shows that the CVS-III data covers the temperature region from 1140 to 1540°C (see insert in Figure 2) with a maximum number of glasses near 1350°C (the T_M of the baseline glass). By comparison, the low temperature phases of the CVS-I and -II were designed around 1150°C.

Table IV. Component effects on processing parameters measured at the CVS3-1 composition.

Effect	SiO_2	B_2O_3	Na_2O	Li_2O	Fe_2O_3	Al_2O_3	ZrO_2	Bi_2O_3	P_2O_5	UO_2	Others
T_M (K)	1,916	-1,546	-1,964	-5,620	-727	1,100	164	-710	642	-344	-698
F_η (10^3 K)	2.1	-63.9	-20.5	-88.3	-7.9	11.1	60.3	-26.2	2.5	-12.7	10.3
$\dot{\varepsilon}_M$ (S/m)	21	-335	211	200	-90	-128	-121	-154	-28		-289
F_ε (10^3 K)	-7.8	8.5	18.1	3.6	-5.6	-1.0	-19.0	-4.8	15.1		7.3
T_g (K)	174	260	-549	-1,696	46	314	265	-658	209		178

The T_M range for CVS-III being 1140 to 1540°C (Figure 2), an addition of any component with a coefficient ≤ 1140 or ≥ 1540°C is likely to decrease or increase T_M, respectively. As Table V shows, components that increase T_M are, Al_2O_3, SiO_2, and P_2O_5; T_M is decreased by Li_2O, Na_2O, B_2O_3, Bi_2O_3, Fe_2O_3, and Others; UO_2 and ZrO_2 can either increase or decrease T_M depending upon the glass composition. The T_M range for CVS-I and -II is 900 to 1450°C. Components that increase T_M of these glasses are Al_2O_3, SiO_2, and ZrO_2; T_M is decreased by Li_2O, Na_2O, CaO, B_2O_3, and MgO; Fe_2O_3 and Others can either increase or decrease T_M depending upon the glass composition.

Many glass components effect T_M of high-temperature (CVS-III) and low-temperature (CVS-I and -II) glasses in a similar manner. The CVS-I and -II coefficients for SiO_2 and Al_2O_3 are virtually identical with those for CVS3-1. Coefficients of the components that tend to decrease T_M (Li_2O, Na_2O, and B_2O_3) have somewhat lower values (stronger effects) in high-temperature glasses. For B_2O_3, this may have resulted from lower concentrations of B_2O_3 in high-temperature glasses in conjunction with boron's nonlinear effect on glass viscosity. Small additions of Li_2O, Na_2O and B_2O_3 may be used to lower T_M when desirable (see further discussion in Section 4.6). The coefficient for Fe_2O_3 is substantially lower in high-temperature glasses, probably because of a higher Fe^{II}/Fe ratio (this has not been confirmed experimentally). As reported by Li et al. (1995), T_M is also decreased by TiO_2 (not included in Tables IV and V).

Table V. First-order model coefficients for the melting temperature, VFT viscosity parameters, Arrhenius viscosity and electrical conductivity parameters (determined from CVS3-1 data and models fit to CVS-I and -II data) and electrical conductivity at melting temperature (determined from CVS3-1 data).

	T_M (K)		ln η (Pa·s)										ln ε (S/m)				ε_M
	(at 5 Pa·s		A		B (10^3K)		T_0 (K)		E		F (10^3K)		E		F (10^3K)		(S/m)
CVS	3-1	I&II	3-1	I&II	3-1	I&II	3-1	I&II	3-1	I&II	3-1	I&II	3-1	I&II	3-1	I&II	3-1
SiO_2	2258	2262	-5.6*	-4.3	18.5	12.0	280*	501	-22.7*	-11.1	23.3*	28.5	8.1	8.1	-11.4	-10.3	58.6*
B_2O_3	-180	610	21.7	-5.6	-56.2	-3.9	2005	1001	14.4*	-13.7	-41.6	10.9	1.0*	12.8	0.7*	-15.1	-286.2
Na_2O	-355	-71	-6.4	-8.0	-7.5	-1.7	500*	494	-15.2	-9.6	4.3	-1.2	7.7	6.1	8.1	7.1	237.5
Li_2O	-4093	-2464	11.3*	-6.1	-72.2	-23.3	1045	512	-7.3*	-4.5	-63.5	-42.3	25.8	7.5	-4.3	22.5	227.9
CaO		331		-13.2		2.0		877		-22.8		21.5		14.4		-18.8	
MgO		686		-13.0		7.9		1270		-21.1		25.8		10.4		-13.4	
Fe_2O_3	688	1179	-7.7*	-6.2	1.5*	5.4	770*	570	-16.6	-6.4	21.0	8.8	11.9*	9.9	-12.9*	-10.6	-41.3
Al_2O_3	2412	2462	-12.7	-2.8	29.0	13.3	314	84	-9.2	-4.1	32.9	21.2	-10.9	7.1	-6.7*	-8.2	-36.4*
ZrO_2	1523	2000	-38.8	-22.3	58.1	27.6	-332	1663	-48.9	-31.3	80.0	54.6	15.8	7.9	-25.9	-9.7	-66.3*
Bi_2O_3	666		-8.2		3.6*		312		-0.1*		-3.5*		2.9*		-12.4*		-44.8
P_2O_5	2203		-10.1*		-10.0*		1080		-2.9*		2.5		0.7		7.3		32.8*
UO_2	1054		14.3*		-20.6*		3331*		-7.0*		-12.7*						
Others	765	1339	-9.7	-9.9	4.9	9.3	808	890	-22.4	-17.0	10.3	23.0	2.1	18.1	-1.5	-20.7	-213.1
Min	1428	1169	-9.2	-9.4	7.7	4.3	425	407	-16.6		19.3		7.9		-10.2		29.8
Max	1822	1727	-6.3	-3.8	14.2	9.8	539	612	-10.23		31.5		10.6		-6.1		76.7

* Indicates highly nonlinear response at CVS3-1 composition as determined from plots of data.

4.2 Vogel - Fulcher - Tammann Relationship

It is valuable to consider the effects of composition on the VFT parameters (A, B, and T_0) for understanding of viscosity at any temperature. The first-order coefficients in Table V were obtained by fitting first-order models (Equation (3)) to the A, B, and T_0 values from Table III (these values were obtained using T_g data along with measured viscosity values except for glasses containing UO_2). These VFT models will be used to:

- formulate optimum glass compositions,
- assess the effects of temperature on melter operation for a given composition,
- estimate effects of composition fluctuations on melter operation, and
- provide means of mitigating operational problems through feed trimming.

The effect of composition on viscosity was described in depth for low temperature glasses by Hrma et al. (1994 and 1995). Note that the first-order coefficients for high-temperature glasses in Table V are strictly valid for the CVS3-1 composition neighborhood. The CVS-I and -II coefficients are averaged over the composition range of low temperature CVS glasses.

The T_0 and A parameters represent extreme values: T_0 is the temperature at which $\eta \rightarrow \infty$

and A is the ln η value at $T \rightarrow \infty$. The experimental data are confined to a narrow range of viscosity and temperature and hence the T_0 and A values are subject to a large uncertainty, which is only partially reduced by using an additional high viscosity data point at T_g. The composition dependence of A is generally weak. It has been suggested that A be taken as a composition independent constant for waste glasses (Hrma et al. 1995).

In the case of the B parameter, its coefficient values for the CVS3-1 glass roughly parallel the averaged B coefficients for low temperature glasses (CVS-I and -II) and also parallel the glass length F_η coefficients determined by fitting the Arrhenius equation to the viscosity data (Section 4.4). ZrO_2 most increases and Li_2O most decreases B. Al_2O_3 and SiO_2 also increase B, whereas Na_2O decreases it. Fe_2O_3 has little effect on B. B_2O_3 decreases B significantly more in CVS3-1 glass than in the low temperature glasses.

4.3 Electrical Conductivity

Like viscosity, electrical conductivity is a function of both temperature and composition. For practical purposes, the effect of composition on the electrical conductivity of glass at the melting temperature (ε_M) is considered. The component effects shown in Table IV and Figure 3 and component coefficients shown in Table V confirm that electrical conductivity is increased only by alkaline oxides, i.e., Na_2O and Li_2O (Hrma et al. 1995). SiO_2 and P_2O_5 have little effect. All other components tend to decrease electrical conductivity.

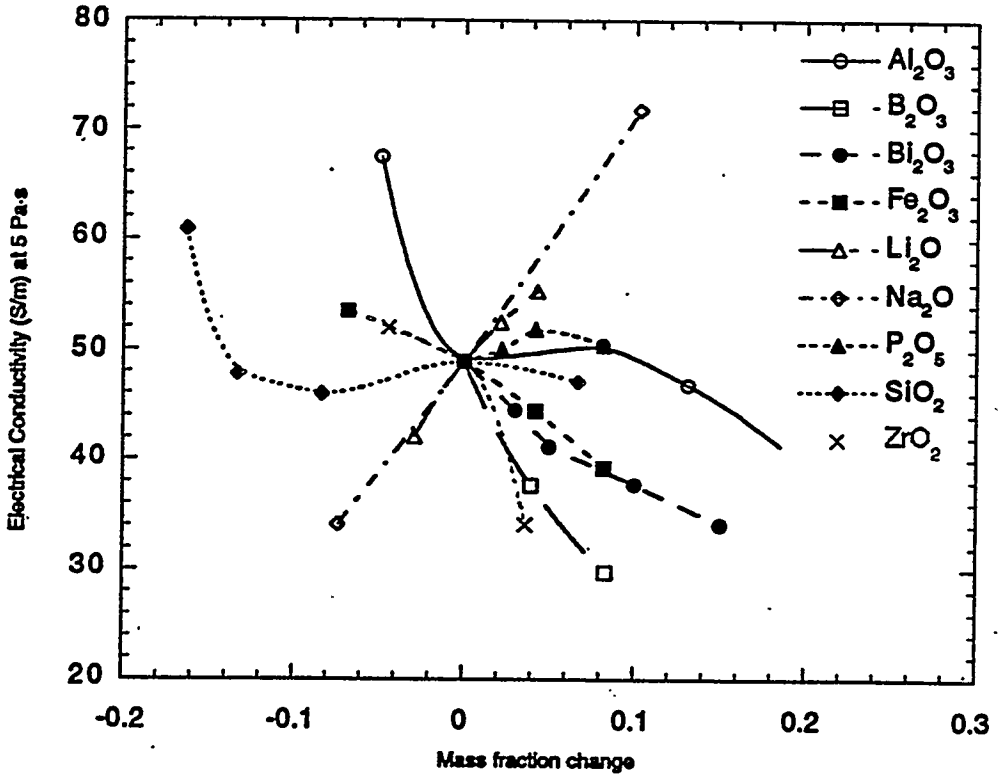

Figure 3 Component effects on electrical conductivity at melting temperature.

4.4 Length

The component effects for activation energy in the Arrhenius equation (Equation (2)) express the effect of components on the response of the glass to changing temperature, i.e., the viscous (F_η) or electrical (F_ε) "length" of glass. According to Table IV, the component that "shortens" CVS3-1 glass most with respect to viscosity is ZrO_2; that which most "lengthens" it is Li_2O. These and the effects of other components on the viscous length are consistent with the effects on VFT B component coefficients discussed in Section 4.2. The electrical conductivity dependence of CVS3-1 glass on temperature is lengthened most by Na_2O followed by P_2O_5 (Table IV). The differences between CVS3-1 glass component coefficients and those of the CVS-I and -II are evident from Table V. Except for B_2O_3, Li_2O and ZrO_2, the values of coefficients are similar.

4.5 Glass Transition Temperature

Figure 4 shows the effect of components on T_g when varied one component at a time from the CVS3-1 glass. It can be seen by this plot that T_g is lowered by the alkaline oxides (Li_2O and Na_2O) and Bi_2O_3, while raised by Al_2O_3, ZrO_2, B_2O_3, Fe_2O_3 and SiO_2. The effect of P_2O_5 on T_g is anomalous. Small additions (2 wt%) of P_2O_5 decrease T_g as much as equivalent additions of Li_2O and Bi_2O_3. Additions larger than 5 wt% have an increasing effect on T_g. This behavior may be related to crystallization of phosphates (see Table VIII). The numerical values of component effects, evaluated as the first derivatives of T_g with respect to mass fraction change at the baseline composition, are reported in Table IV. Similar relative component effects are seen in low temperature glasses as evident by the average low temperature component coefficients.

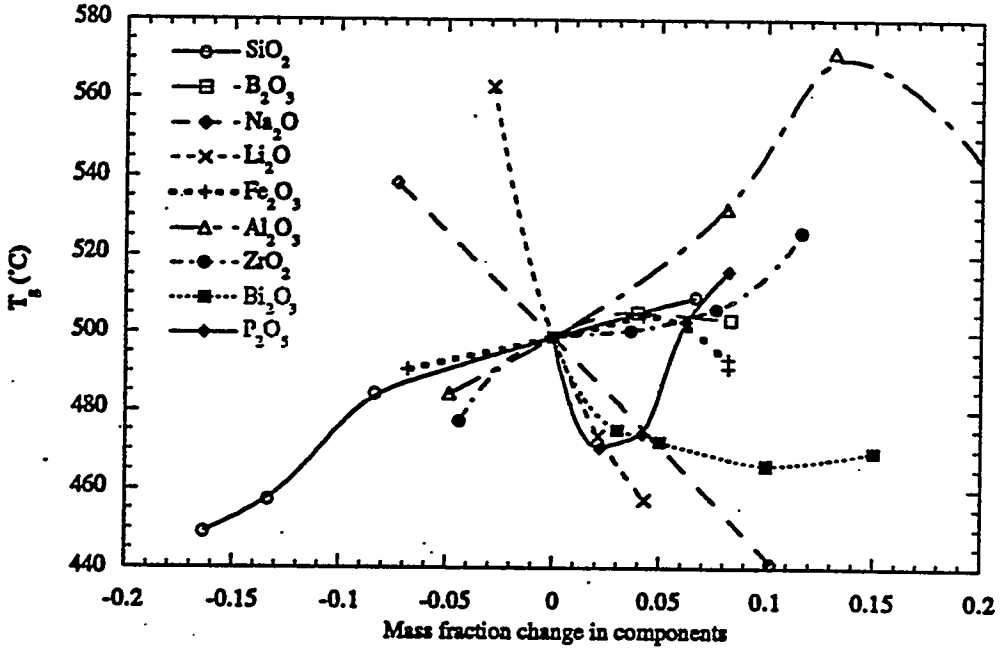

Figure 4. Component effects on T_g.

It is interesting to compare the difference in components effects on T_g to those on T_M (Table IV) since T_g and T_M represent the temperature at a constant viscosity, $10^{11.3}$ and 5 Pa.s, respectively. Both temperatures are decreased most by Li_2O and also by Bi_2O_3 and Na_2O. The T_M is increased most by SiO_2, Al_2O_3, and P_2O_5, while T_g is increased most by Al_2O_3, ZrO_2, and P_2O_5. SiO_2 has a much stronger effect on T_M than T_g. The effect of B_2O_3 and Fe_2O_3 are opposite for T_M and T_g.

4.6 Liquidus Temperature

Glass can crystallize at $T < T_L$. Crystalline phases, if precipitated in some types of melters, such as a continuous melter with a flat bottom, can cause sludge formation on the melter bottom or even melter electrode shorting if the phases are highly conductive. For these reasons, restrictions have been placed on glass to avoid precipitation and sludge formation in the melter. Since this behavior is difficult to predict, restrictions on composition must be conservative to avoid the problematic events. To better predict T_L of glass, a fundamental understanding of the phenomena and composition effects must be gained.

The T_L's of CVS III glasses are listed in Section 10.4. The effects of components on the T_L of CVS3-1 glass are shown in Figure 5 and summarized in Table VI.

Table VI. Effect of components on T_L, T_M, and T_M-T_L of CVS3-1 glass.

Effect	SiO_2	B_2O_3	Na_2O	Li_2O	Fe_2O_3	Al_2O_3	ZrO_2	Bi_2O_3	P_2O_5	Others
T_L (K)	337	-305	-2,094	-3,609	1,663	1,699	688	-289	708	556
T_M (K)	1,916	-1,546	-1,964	-5,620	-727	1,100	164	-710	642	-698
T_M - T_L (K)	1,584	-761	48	-2,011	-2,099	-599	-544	-421	-67	-1,474

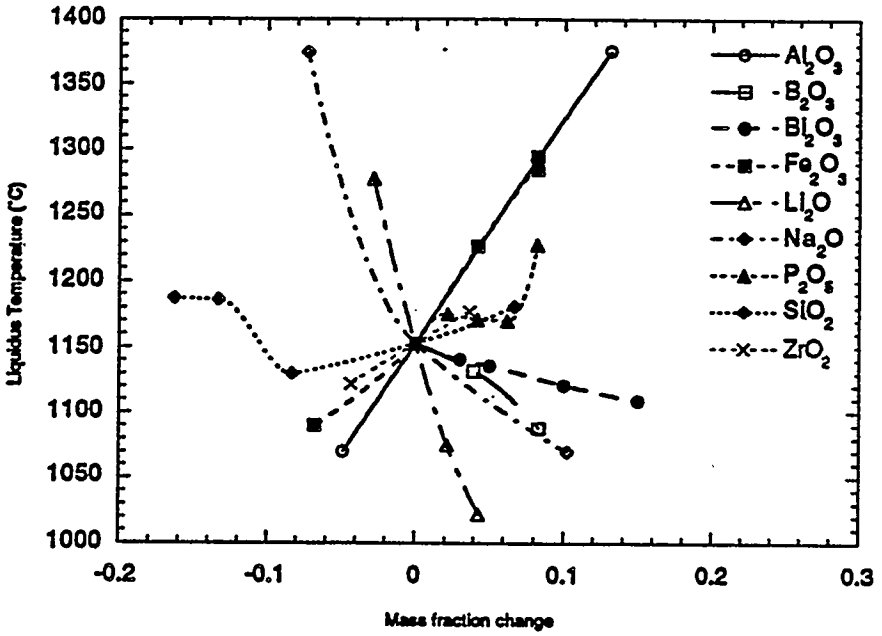

Figure 5. Component effects on T_L.

As Figure 5 shows, the effects of most components on T_L are linear. The deviation from linearity seen in SiO_2 and P_2O_5 effects is caused by a change in the primary phase of crystallization. For a majority of the CVS-III glasses, spinel was the primary phase, see Section 10.4. For low SiO_2 glasses, the primary phase is neodymium-cerium-zirconate. The highest P_2O_5 glass has a primary phase of rare earth (Nd, La, and Ce) zirconate. For eight glasses, T_L was not obtained. Five of these glasses contain UO_2 (CVS3-32 to -36) and the remaining three contain 25 and 18 wt% Al_2O_3 and 16 wt% ZrO_2 (CVS3-16, -17, and -20).

The T_L of CVS3-1 glass with a spinel primary phase is increased most by Fe_2O_3 and Al_2O_3, followed by P_2O_5, ZrO_2, Others and SiO_2. It is most decreased by Li_2O and Na_2O, followed by B_2O_3 and Bi_2O_3.

Examining the effect of each component on the difference between T_M and T_L (Table VI) shows that addition of SiO_2 most effectively increases the gap between melting and liquidus temperatures. This follows from the ability of SiO_2 to increase the glass forming tendency. This positive effect of SiO_2 on T_M-T_L elucidates the empirical observation that high-temperature HLW glasses generally allow a higher waste loading compared to low-temperature glasses (as a rule, SiO_2 is the only additive needed in high-temperature HLW glasses). Na_2O has little effect on T_M-T_L whereas additions of Li_2O and B_2O_3 decrease T_M-T_L. If T_M must be reduced, it is therefore advantageous to use Na_2O as a viscosity reducing additive rather than Li_2O or B_2O_3. This agrees with the conclusions of Kim et al. (1994). T_M-T_L is strongly decreased by adding refractory oxides (Fe_2O_3, Al_2O_3, and ZrO_2) and by Others which contain crystal forming components NiO, Cr_2O_3 and CeO_2.

Table VII. First-order model coefficients for spinel liquidus temperature.

Coefficient (K)	SiO_2	B_2O_3	Na_2O	Li_2O	CaO	MgO	Fe_2O_3	Al_2O_3	ZrO_2	Bi_2O_3	P_2O_5	Others
CVS3-1	1,282	1,121	-409	-2,080			2,976	3,042	2,084	1,141	2,128	1,905
CVS-I and -II	1,262	939	277	144	1,639	3,103	2,529	2,008	1,201			1,278

First-order model coefficients of spinel T_L, presented for CVS3-1 glass and for CVS-I and -II glasses in Table VII, show a good agreement between low- and high-temperature glasses. Na_2O and Li_2O decrease T_L more strongly in high- than in low-temperature glasses. The refractory oxides also seem to exhibit somewhat stronger effects.

5.0 Product Characterization

Results from PCT testing of the CVS-III glasses are given in Section 10.5. For borosilicate glasses, the normalized boron release is commonly used as the indication of network dissolution by PCT because B_2O_3 is a glass forming oxide (in alkali containing glasses) and once in solution, it doesn't precipitate in secondary phases. However, B_2O_3 concentrations in high-temperature HLW glasses can be very low, thus giving small releases subjected to large measurement errors. Since this is true for a majority of glasses in this study, sodium release was used instead of boron release as a glass durability measure in this report. Na_2O is present in large concentrations in all Hanford HLW glasses. As CVS-I and -II data show, Na and B normalized releases are generally close to each other (Hrma, Piepel et al. 1994). Although Na^+ is subjected to initial ion exchange between glass and water and can participate in secondary reactions, these effects are generally small.

Table VIII. Component effects on ln r_{Na}.

Effect	CVS3-1	HW39-4	WV205	HTB651	PFP	CVSI&II
SiO_2	-4.45	-11.75	-6.08			-10.61
B_2O_3	-9.48	10.47				9.93
Na_2O	27.23	32.52	5.76*			21.28
Li_2O	12.20	42.00	5.78*			19.27
CaO		16.33				-2.49
MgO		42.10				11.40
Fe_2O_3	-4.11		18.01			-4.97
Al_2O_3	-17.34	-42.95	-14.23			-26.56
ZrO_2	-7.79		-8.85			-12.42
Bi_2O_3	0.42					
P_2O_5	-5.91			-11.21	-12.44	
UO_2	-0.73					
Cr_2O_3			17.12	11.33		
TiO_2			-21.89	-5.03		
Others	-0.97					-1.26

* WV205 with 3wt% Al_2O_3 addition was used as baseline for alkaline oxides.

The component effects taken as slopes of component change versus ln r_{Na} at the zero change point (CVS3-1 glass) are listed in Table VI. These effects are compared for different baseline glasses and composition regions: HW39-4 (Hrma, Piepel et al. 1994), WV205 (Feng et

al. 1989), HTB651 (Li et al. 1995), PFP (Li et al. 1995), and CVS-I and -II region (taken at the HW39-4 composition).

In Table VIII, CVS3-1 and HTB651 are high-temperature glasses while all others melt at 1150°C. Component effects for high- and low-temperature glasses show similar trends except for B_2O_3, which increases r_{Na} (decreases durability) in low-temperature glasses and decreases r_{Na} (increases durability) in high-temperature glasses. The magnitude of SiO_2 effect is lower in the high-temperature CVS3-1 glass than in low-temperature glasses.

Comparing CVS-I and -II and HW39-4 component effects shows significant differences between averaged and local values for Li_2O, CaO, and MgO. Li_2O has definitely a much stronger effect on the HW39-4 glass (see Section 5.3) compared to the average low temperature effect (Hrma, Piepel, et al. 1994). The effect of CaO is taken from one data point at 1.17 wt% addition and thus is subject to experimental uncertainty. The difference in the effect of MgO is considered real—see discussion in Hrma, Piepel, et al. (1994).

The beneficial effect of P_2O_5 on CVS3-1 glass durability is comparable to that obtained for HTB651 and PFP glasses. Two more component effects are shown in Table VIII from the HTB651 series: Cr_2O_3 and TiO_2. Cr_2O_3 substantially increases sodium release (decreases durability) as confirmed by WV205 series and low-level waste glass data (Li 1995). However, this effect has low practical consequence because of the low Cr_2O_3 solubility in waste glasses. TiO_2 decreases sodium release (increases durability) but to a lesser extent than Al_2O_3 and ZrO_2. Positive effect of TiO_2 on glass durability of high-sodium glasses which is weaker than the effect of Al_2O_3 was shown in a literature review by Kim and Hrma (1995).

Components effects obtained from Feng's (1989) data for WV205 glass are also shown in Table VIII. The effects of Al_2O_3, ZrO_2 and Cr_2O_3 are in reasonable agreement with the values for other glasses. The effects of Fe_2O_3 and TiO_2 were based on one and two data points, respectively, in addition to the baseline glass. These effects are probably subjected to experimental error. Additionally, it is not clear from Feng's paper whether the Fe_2O_3 enriched glass was prepared under the same redox conditions as the baseline glass.

5.1 SiO_2

The effect of silica on glass durability is positive. As a strongly-bonded network former, SiO_2 increases glass network connectivity. A decrease in r_{Na} with increasing SiO_2 concentration is seen in Figure 6. The effect of SiO_2 on ln r_{Na} as measured at CVS3-1 is -4.45 which is lower than that measured at WV205 (-6.08) and HW39-4 (-11.75) compositions. The difference in effects between the high-temperature glass (CVS3-1) and the low-temperature glass (HW39-4) is remarkable: SiO_2 addition effect the low-temperature glass more strongly. Both glasses have the same mass fractions of SiO_2 (0.533) and $Na_2O + Li_2O$ (0.150) and similar content of Fe_2O_3 and ZrO_2. They differ in concentrations of B_2O_3 (0.0005 for CVS3-1 and 0.105 for HW39-4) and Al_2O_3 (0.049 for CVS3-1 and 0.024 for HW39-4). These differences in composition result in higher durability and viscosity of the high-temperature glass. Whether these composition differences cause the difference in SiO_2 effect on PCT release is unclear. The effect of CCC is not seen in either glass until a very low SiO_2 concentration where crystallization has degraded glass durability.

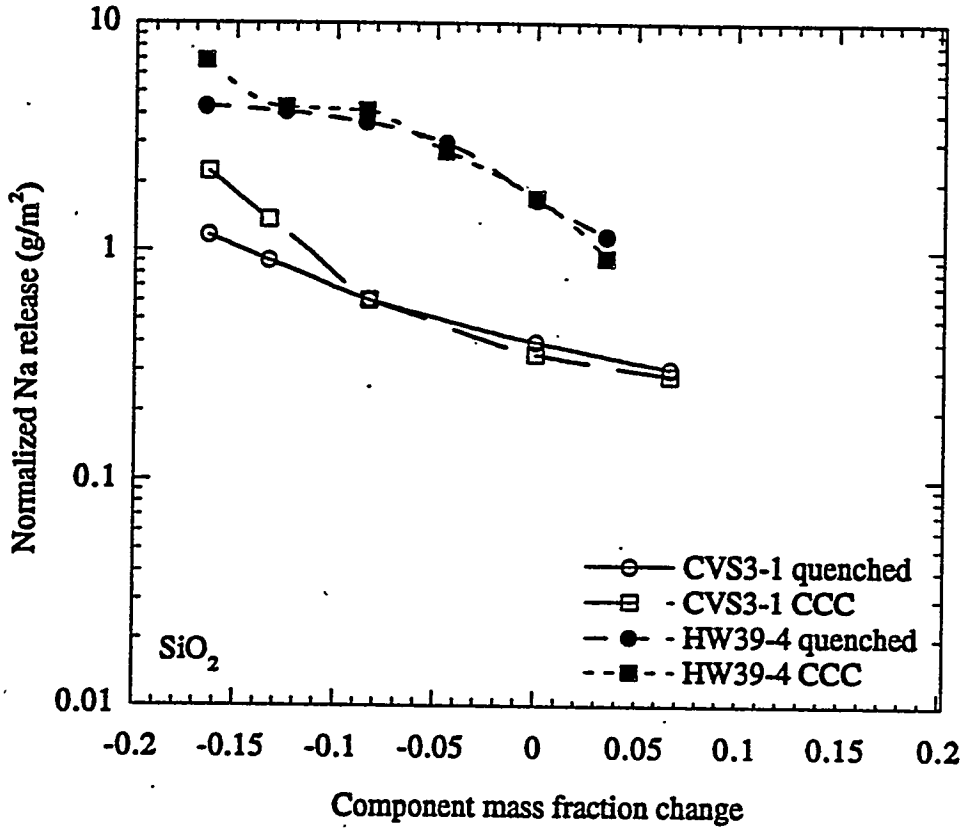

Figure 6. Normalized Na release from 7-day PCT of quenched and CCC glasses as a function of SiO_2 concentration.

5.2 Na_2O

In a silicate glass, sodium is incorporated as a Na^+ ion which is charge-compensated by the creation of a non-bridging oxygen (NBO) ion. The creation of NBO's in a silicate glass lowers network connectivity and degrades durability. However, the specific (or quantitative) effect of Na_2O varies with overall glass composition due to interactions with Al_2O_3, B_2O_3 and other components (DeYoreo and Navrotsky 1990). Na_2O also affects glass redox (Schreiber et al. 1994) and would affect the durability of glasses with high concentrations of transition metals such as iron. The indirect effect of redox may not be seen in these glasses because the glass is unable to reach redox equilibrium with air during the short melting period (2 hour) used to fabricate all glasses in this study.

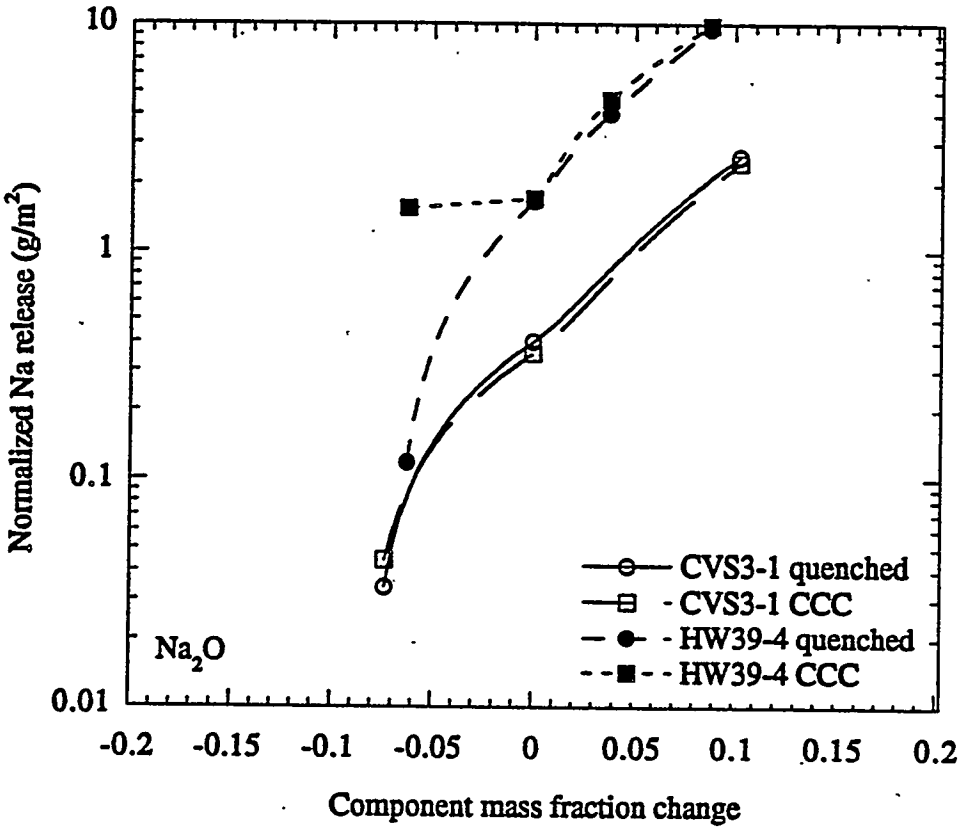

Figure 7. Normalized release from 7-day PCT of quenched and CCC glasses as a function of Na_2O concentration.

Figure 7 displays the effect of Na_2O on the r_{Na} of CVS3-1 and HW39-4 glasses. The effect of Na_2O on ln r_{Na} as measured at CVS3-1 is 27.23 which is somewhat lower than that measured at HW39-4 composition (32.52). The effect of CCC is evident in the less durable HW39-4 glass with the lowest Na_2O concentration. This glass is susceptible to amorphous phase separation which likely caused the decrease in CCC glass durability (Peeler and Hrma 1994).

5.3 Li_2O

Like Na_2O, Li_2O decreases glass durability by creating NBO's and loosening the glass network. All interactions discussed for Na_2O also apply to Li_2O, plus an additional interaction known as the mixed alkali effect. This is a nonadditive effect of combined alkaline oxides on a glass property and is generally.

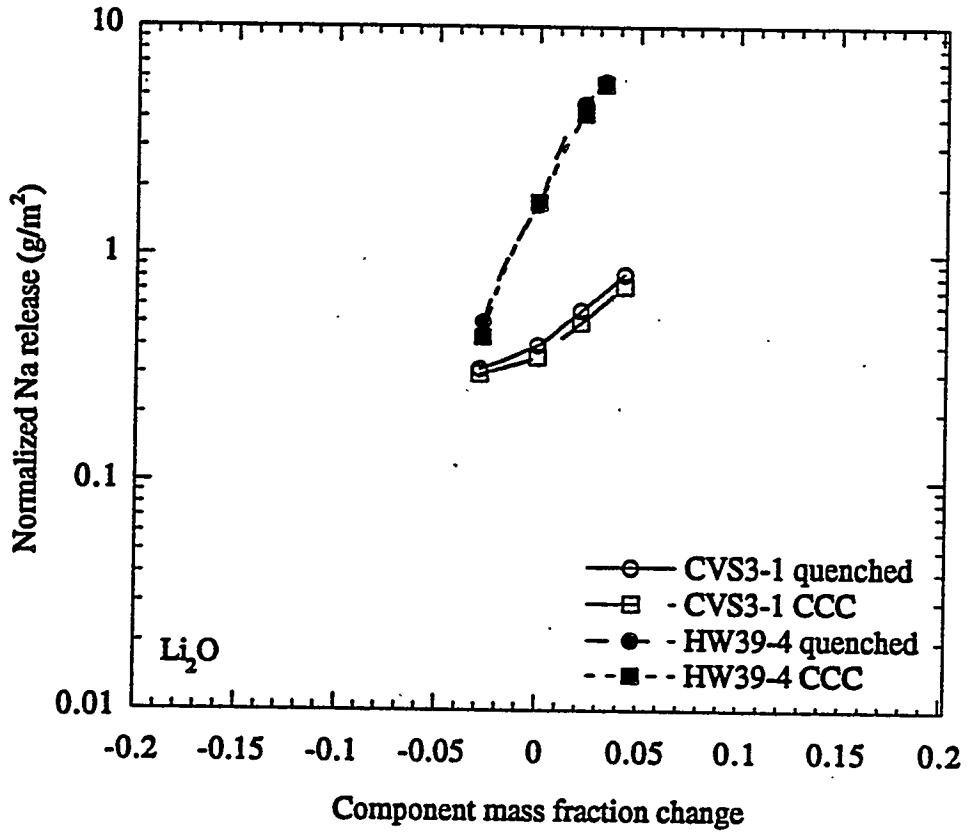

Figure 8. Normalized release from 7-day PCT of quenched and CCC glasses as a function of Li_2O concentration.

Figure 8 displays the effect of Li_2O on the r_{Na} of CVS3-1 and HW39-4 glasses. The effect of Li_2O on ln r_{Na} as measured at CVS3-1 is 12.20 which is significantly lower than that measured at HW39-4 composition (42.00). The averaged effect of Li_2O (in CVS-I and -II) is 19.27. The large differences in Li_2O effect from one baseline glass to another are in sharp contrast with the effect of Na_2O which does not change significantly from glass to glass, suggesting interactions of Li_2O with other glass components such as B_2O_3 and Al_2O_3 (see discussion in Section 5.1). CCC treatment didn't markedly change the r_{Na} of these glasses.

5.4 B_2O_3

Boron can enter a silicate glass as a network forming BO_4^- ion which is normally charge-compensated by association with an alkali atom. Although BO_4^- is not bonded as strongly as SiO_2 tetrahedra (or as durable) in a silicate network, its association with Na^+ is electrostatic and, hence, stronger. Bunker (1994) reports that BO_4^- and AlO_4^- sites are five orders of magnitude more resistant to ion exchange than NBO sites. Due to this decrease in NBO concentrations, B_2O_3 improves glass durability at low to moderate concentrations (usually up to 6 wt%). Excessive concentration of B_2O_3 enters the glass network in threefold coordination which doesn't lower

NBO concentrations and decreases network strength (Volf 1984). As the relative alkali concentration is increased, the B^4:B^3 ratio reaches a maximum, and then decreases; this is known as the boron anomaly (LaCourse and Stevens 1977). In general, B_2O_3 increases glass durability at low concentrations and decreases durability at high concentrations. This effect has been demonstrated by replacing SiO_2 by B_2O_3 (Kim 1994) or Na_2O by B_2O_3 (Bunker 1987) in simple glass compositions.

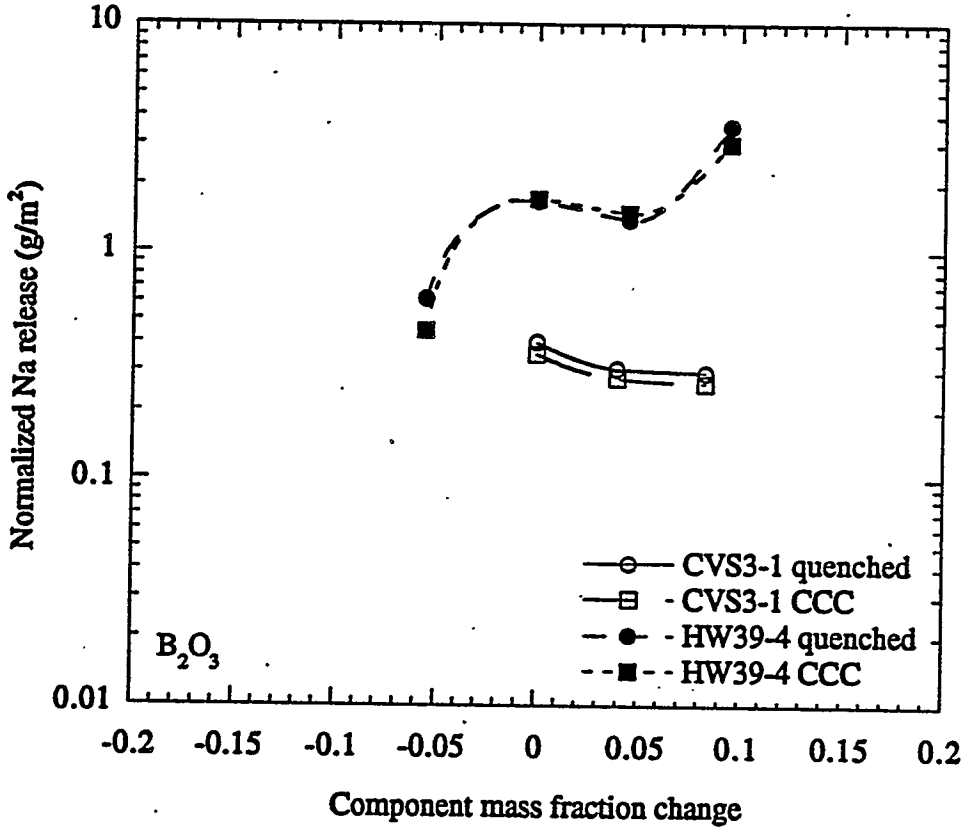

Figure 9. Normalized release from 7-day PCT of quenched and CCC glasses as a function of B_2O_3 concentration.

Figure 9 displays the effect of B_2O_3 on the r_{Na} of CVS3-1 and HW39-4. The strong nonlinear effect of boron is demonstrated by the differences between the measured effects at each baseline composition: -9.48 at CVS3-1 ($g_{B_2O_3} = 0.0005$) and 10.47 at HW39-4 ($g_{B_2O_3} = 0.1048$). This effect is also shown by the curvature of the second-order model predictions (Hrma, Piepel, et al., 1994).

5.5 Fe_2O_3

The effect of iron on glass durability depends on the redox state of the glass. In general, addition of Fe_2O_3 increases glass durability while FeO decreases durability. Fe_2O_3 may also enter the network in four- and six-fold coordination and is prone to association with alkali ions (Volf,

1984). Figure 10 displays the effect of Fe_2O_3 on the r_{Na} of CVS3-1. The effect of Fe_2O_3 on ln r_{Na} as measured at CVS3-1 is -4.11. The effect of Fe_2O_3 on HW39-4 has not been measured. The averaged effect of Fe_2O_3 on CVS-I and -II glasses is virtually the same (-4.97) as that for the CVS3-1 glass. CCC treatment effects on the durability of the CVS-III iron glasses result from crystallization as described in Section 5.12.

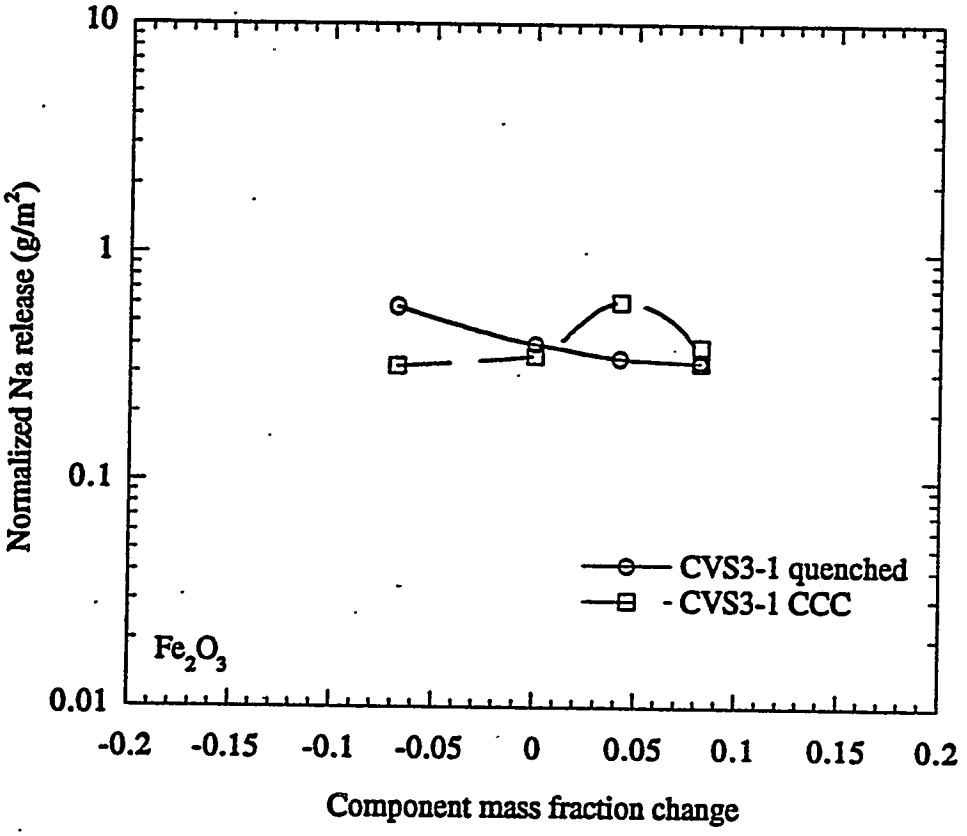

Figure 10. Normalized release from 7-day PCT of quenched and CCC glasses as a function of Fe_2O_3 concentration.

5.6 Al_2O_3

Like B_2O_3, Al_2O_3 increases glass durability by decreasing NBO concentration. Al_2O_3 is strongly bonded to the glass network in both four- and six-fold coordinations. Hence, Al_2O_3 has not been seen to decrease the durability (by 7-day PCT) of glasses. The positive effects of Al_2O_3 are generally more dramatic in glasses with low network former and high alkali concentrations. Figure 11 displays the effect of Al_2O_3 on the r_{Na} of CVS3-1 and HW39-4 glasses. The effect of Al_2O_3 on ln r_{Na} as measured at CVS3-1 is -17.34 which is lower than that measured at HW39-4 composition (-42.95) and similar to than that measured at the WV205 composition (-14.23). The curvature of the ln r_{Na} versus Al_2O_3 change line shows a nonlinear effect which is strongest (accidentally) near baseline compositions.

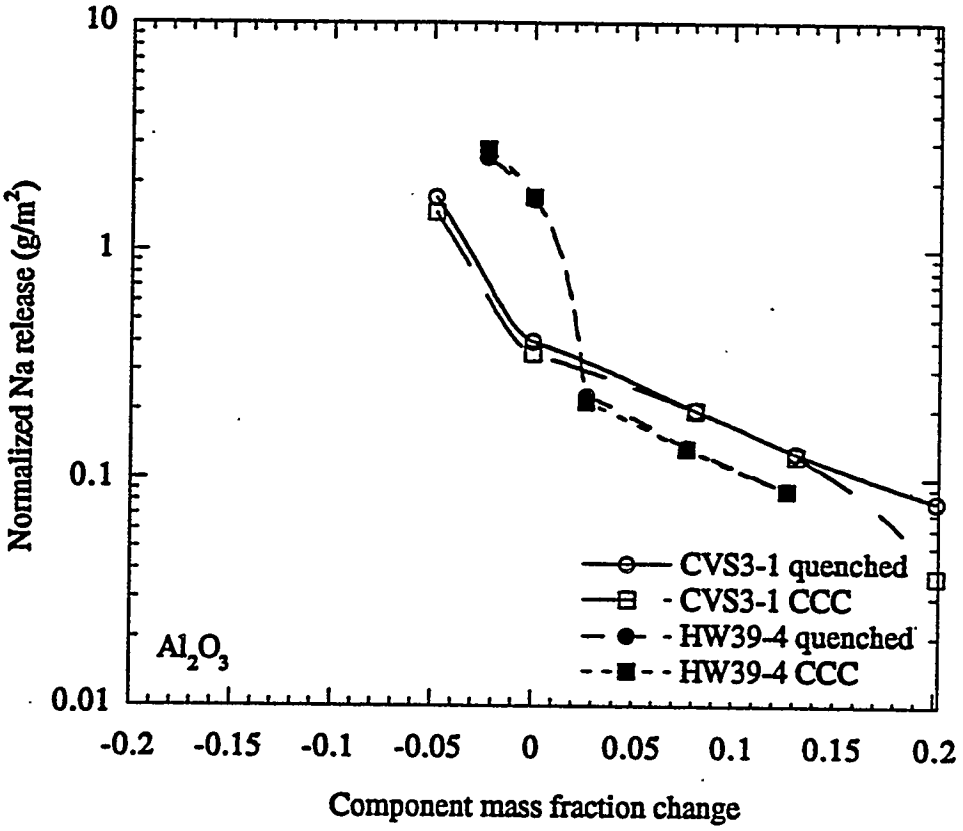

Figure 11. Normalized release from 7-day PCT of quenched and CCC glasses as a function of Al_2O_3 concentration.

Interestingly, Figure 11 demonstrates that a small increase in Al_2O_3 content would significantly improve the durability of HW39-4 glass. Unexpectedly, the Al_2O_3 enriched HW39-4 glass exhibited somewhat higher durability than the CVS3-1 glass with the same addition of Al_2O_3. The plot implies that the effect of Al_2O_3 may not be accurately described by a second-order model over large composition regions, although the approximation could be satisfactory. At higher Al_2O_3 concentrations, the effect is virtually linear with similar slopes for CVS3-1 (-8.11) and HW39-4 (-9.45). CCC treatment of the CVS3-16 glass (25 wt% Al_2O_3) resulted in nearly complete crystallization. The glass ceramics produced had an improved durability over quenched glass (with less than 4 vol% crystalline phases).

5.7 ZrO_2

ZrO_2, like SiO_2 is a network forming component in glass and generally increases glass durability. The effect of ZrO_2 on r_{Na} of the CVS3-1 baseline glass is shown in Figure 12 (it was not measured for HW39-4 glass). The apparent effect of ZrO_2 on the r_{Na} of this glass is nonlinear, however this has not been seen in previous empirical modelling of glass durability. Sample analysis disclosed undissolved ZrO_2 in the 12 and 8 wt% ZrO_2 samples (two highest change data points) which may account for the apparent nonlinearity. The effect of ZrO_2 on ln r_{Na} as measured

at CVS3-1 is -7.79 which is similar to that measured at WV205 (-8.85) and somewhat lower than the averaged CVS-I and -II effect (-12.42). CCC treatment increased the release of the two highest ZrO_2 glasses.

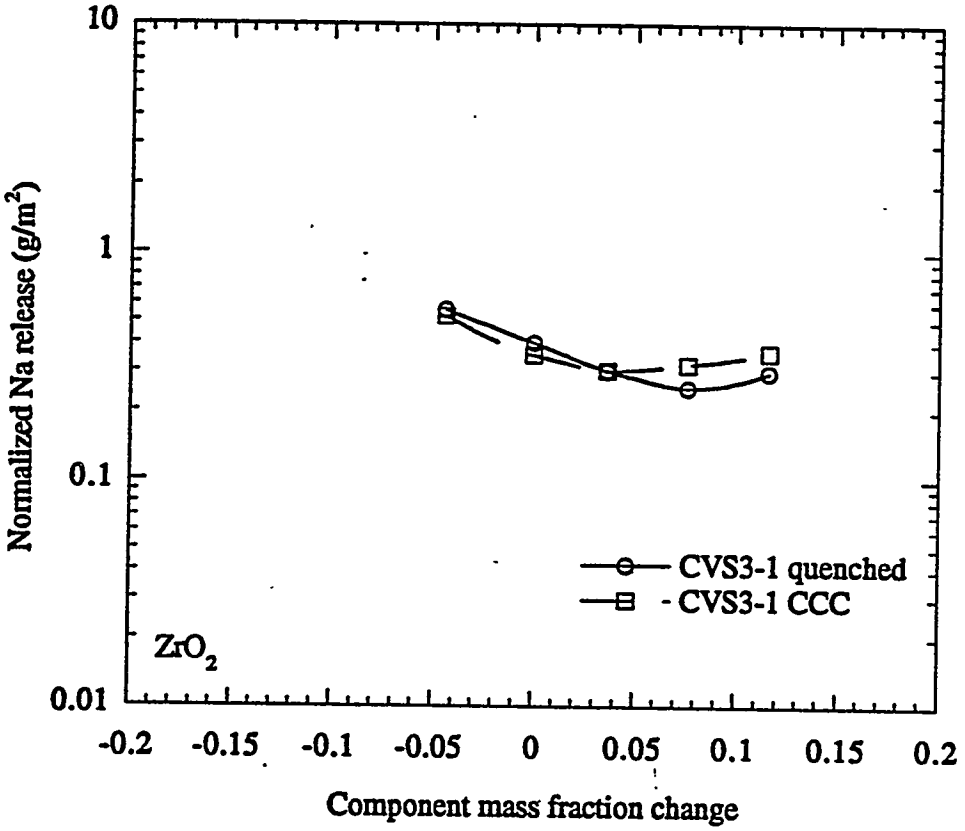

Figure 12. Normalized release from 7-day PCT of quenched and CCC glasses as a function of ZrO_2 concentration.

5.8 Others

The pseudo-component Others (including small concentrations of Bi_2O_3 and P_2O_5) was also varied in this study. This component consists of a mixture of minor waste components which are not thought to have a significant effect on glass durability if Others remains in low concentration in glass. The concentrations of Others was increased to 20 wt% in the baseline glass to ensure this particular Others composition (from all-blend waste, see Section 10.1) would not significantly affect the durability of glass at very high waste loadings. Figure 13 displays the effect of Others on the r_{Na} of CVS3-1. The effect of Others on ln r_{Na} as measured at CVS3-1 is -0.97. The assumption of Others having little effect on glass PCT is upheld by this data.

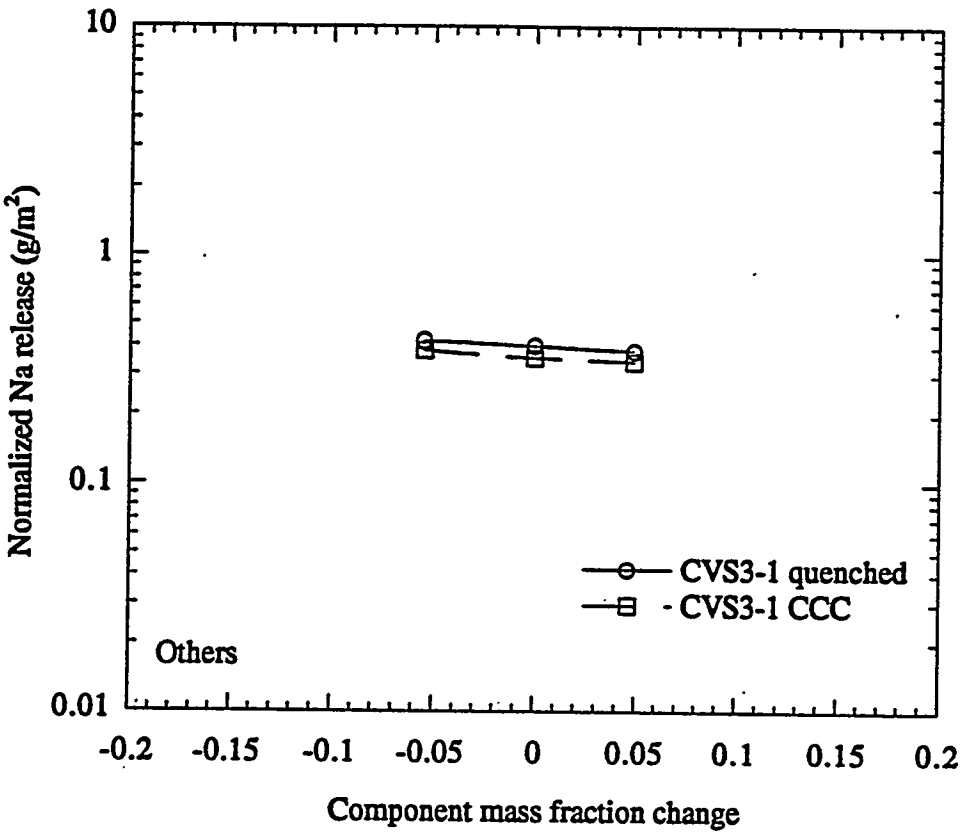

Figure 13. Normalized release from 7-day PCT of quenched and CCC glasses as a function of Others concentration.

5.9 Bi_2O_3

Bi_2O_3 is a network modifying component in glass and affects glass properties much like PbO. Bi_2O_3 is capable of lowering glass viscosity while not degrading glass durability. Although Bi_2O_3 has not been considered as an additive for nuclear waste vitrification, its presence in waste is generally helpful to glass formulation. Figure 14 displays the effect of Bi_2O_3 on the r_{Na} of CVS3-1. A slight increase in r_{Na} is seen with increasing concentration. The effect of Bi_2O_3 on glass durability as measured at CVS3-1 is 0.42 the effect of Bi_2O_3 is not available for HW39-4 or WV205 compositions. The r_{Na} of these glasses was decreased slightly by CCC treatment.

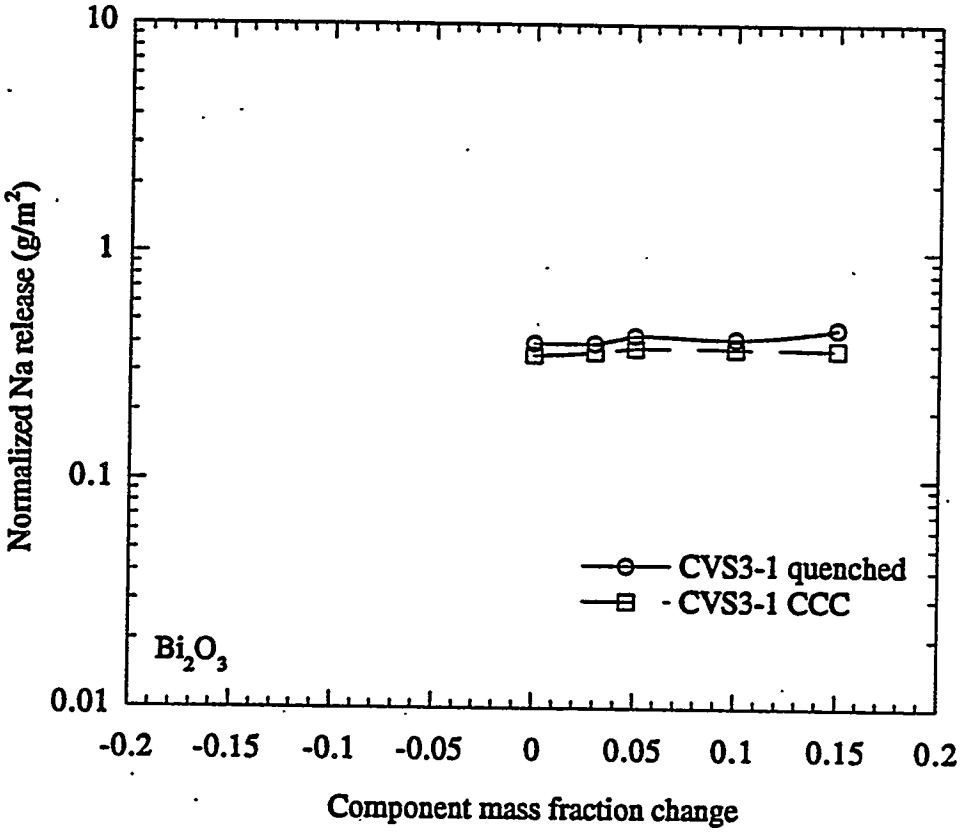

Figure 14. Normalized release from 7-day PCT of quenched and CCC glasses as a function of Bi_2O_3 concentration.

5.10 P_2O_5

Phosphate is a glass forming component. In an alumino-boro-silicate glass, however, the solubility of P_2O_5 is limited. Al_2O_3 has been used to increase phosphate solubility in silicate glasses. However, in boro-silicate glasses the incorporation of P_2O_5 is enabled by Na_2O because Al_2O_3 competes for Na with P_2O_5, Al_2O_3 lowers P_2O_5 solubility in these glasses. Discussion of P_2O_5 in waste glass is given by Li (1995). Figure 15 displays the effect of P_2O_5 on the r_{Na} of CVS3-1. A decrease in r_{Na} is seen with increasing concentration. The effect of P_2O_5 on glass durability as measured at CVS3-1 is -8.42, which is similar to that measured at HTB651 (-11.17) and PFP (-12.44) glasses. The effect of P_2O_5 is not available for HW39-4 or WV205 compositions.

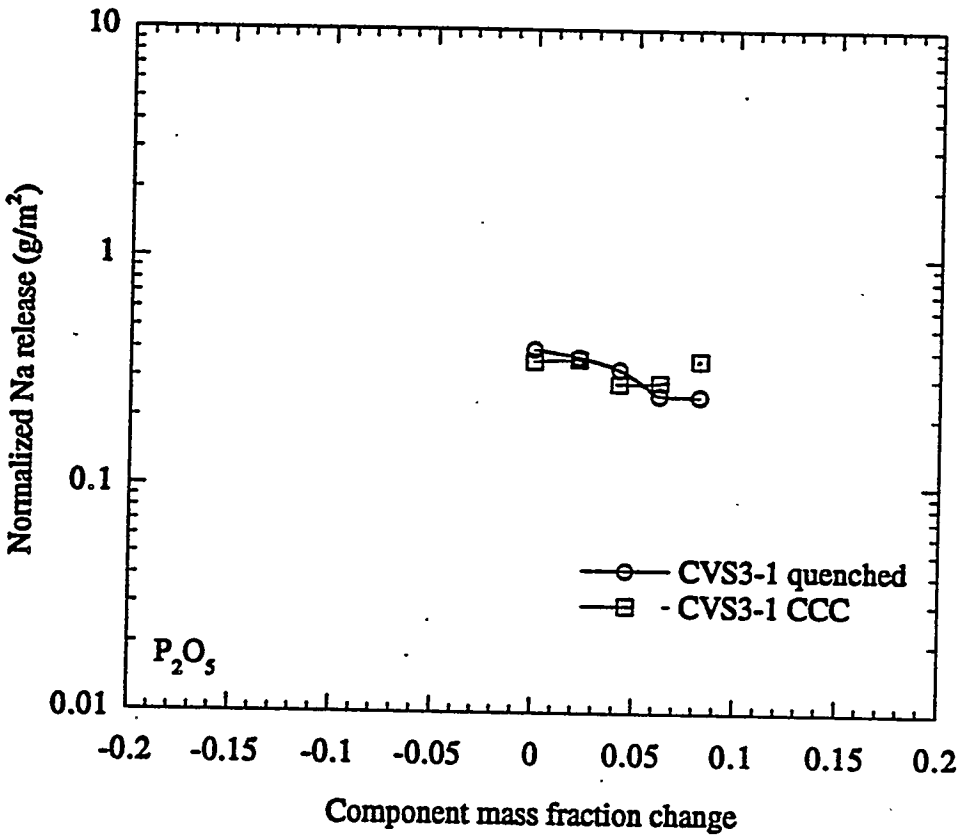

Figure 15. Normalized release from 7-day PCT of quenched and CCC glasses as a function of P_2O_5 concentration.

5.11 UO_2

Uranium enters the glass network in three oxidation states U^{IV}, U^{V}, and U^{VI}, of which U^{VI} has the highest solubility in glass (Schreiber and Balazs 1982). Glasses melted in an oxidizing atmosphere with high U concentrations, such as those considered in this study, will contain an oxide of U^{VI}. However, U was batched in these glasses as U^{IV} and is therefore reported as UO_2.

Uranium is found in high concentrations in the tank waste at Hanford and will likely be seen in all HLW glasses. The cost of glass testing has prohibited the use of U in simulated glasses tested for CVS. Nd_2O_3 was used as a uranium surrogate in a majority of glass testing. One purpose of this study is to evaluate the use of Nd_2O_3 as a uranium substitute.

As seen in Figure 16, UO_2 has little effect on the r_{Na} of CVS3-32, which was the baseline for UO_2 containing glasses (see Section 3.0). The effect of UO_2 on ln r_{Na} as measured at CVS3-32 is -0.73, the effect of UO_2 is not available for HW39-4 or WV205 compositions. CCC had little effect on the r_{Na} of these glasses. Replacing Nd in CVS3-1 by U in CVS3-32 resulted in a change in r_{Na} from 0.400 to 0.326 g/m², respectively.

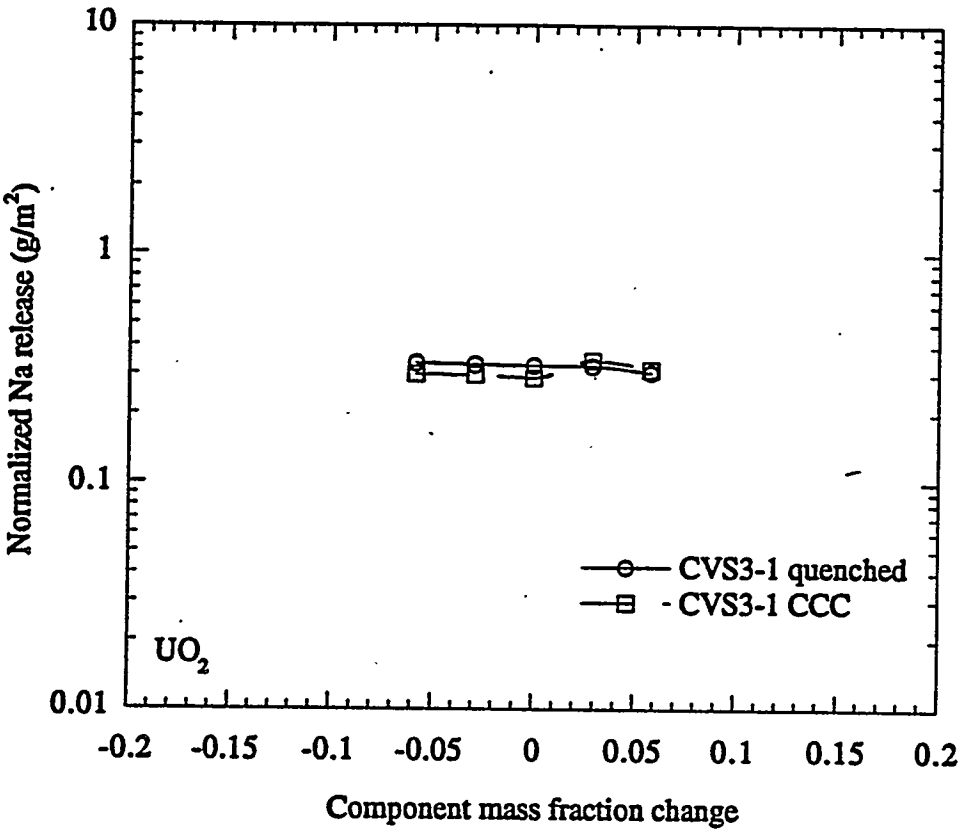

Figure 16. Normalized release from 7-day PCT of quenched and CCC glasses as a function of UO_2 concentration.

5.12 First-Order Model Coefficients

First-order model coefficients for the release of Na, Si, and Li are given in Table IX. The CVS-III coefficients were obtained by applying least squares regression to the whole set of CVS-III data including CVS3-26 (the CVS internal standard glass). The CVS3-1L coefficients were obtained from linear regression of the ln r_i versus component change for individual components. The data were critically evaluated and outliers were deleted. The slopes where transformed to component coefficients by Equation (4) in which predicted response values were used for the baseline composition. The CVS3-1Q coefficients and those for HTB651, HW39-4 and PFP series were obtained in the same way except the slopes were calculated at the baseline composition from a second-order polynomial fit to experimental data. Where the second-order polynomial was not applicable, the CVS3-1L method was used (italicized).

The CVS3-1Q coefficients are equivalent to partial specific property values (Hrma and Robertus 1993). Their validity is restricted to a close neighborhood to the CVS3-1 composition. The CVS3-1L coefficients are averaged values over most of the CVS-III composition region (see Table I). Elimination of outliers and/or anomalous data might shrink this composition region

somewhat. The CVS-III coefficients, taken from Piepel et al. (1995b), are based on a common predicted response value for the baseline composition.

The coefficients in Table IX can be used to calculate predicted PCT releases from glass compositions within their appropriate composition regions. Which coefficients (whether CVS-III or CVS3-1L) give better predictions cannot be determined until model validation is performed. Figures 17 and 18 show that some components exhibit significant nonlinear response. A systematic application of first- and second-order model techniques to all CVS data is provided by Piepel, et al. (1995b).

Table IX. First-order component coefficients for PCT logarithmic normalized sodium (a), silicon (b) and lithium (c) releases from quenched glasses.

(a)

ln(rNa)	CVS-III	CVS3-1L	CVS3-1Q	HTB651	HW39-4	PFP
SiO_2	-3.83	-6.66	-3.02		-4.88	
B_2O_3	0.11	-4.53	-10.39		9.57	
Na_2O	19.05	22.98	22.96		29.31	
Li_2O	13.39	12.74	12.75		40.98	
CaO					*16.71*	
MgO					42.26	
Fe_2O_3	-4.07	-3.97	-4.75			
Al_2O_3	-9.80	-11.89	-17.07		-41.94	
ZrO_2	-5.42	-8.64	-8.43			
Bi_2O_3	-0.31	-0.01	-0.50			
P_2O_5	-7.46	-7.01	-6.76	*-11.58*		*-15.56*
UO_2	-4.03	-1.86	-1.78			
Cr_2O_3				*10.56*		
TiO_2				-5.76		
Others	-3.97	-1.71	-1.76			

(b)

ln(rSi)	CVS-III	CVS3-1L	CVS3-1Q	HTB651	HW39-4	PFP
SiO2	-3.02	-5.01	-3.21		-2.92	
B2O3	-0.61	-2.53	-4.31		0.13	
Na2O	6.85	8.52	6.07		11.09	
Li2O	12.19	13.30	11.92		37.35	
CaO					*6.26*	
MgO					17.93	
Fe2O3	-3.20	-3.57	-3.03			
Al2O3	-5.48	-15.70	-17.00		-29.83	
ZrO2	-7.47	-10.18	-9.94			
Bi2O3	-1.42	-0.30	0.32			
P2O5	-6.44	-4.12	-4.52	*-3.64*		-4.29
UO2	-3.34	-0.95	-1.02			
Cr2O3				*10.50*		
TiO2				-1.90		
Others	-0.30	-2.38	-2.42			

(c)

ln(rLi)	CVS-III	CVS3-1L	CVS3-1Q	HW39-4	PFP
SiO2	-1.95	-3.42	-1.68	-4.02	-
B2O3	0.66	-2.17	-7.62	10.62	
Na2O	*6.74*	8.48	7.36	19.50	
Li2O	13.16	9.15	11.85	38.13	
CaO				*12.26*	
MgO				36.45	
Fe2O3	-3.40	-4.59	-3.59		
Al2O3	-2.06	-11.51	-13.37	-35.76	
ZrO2	-4.54	-6.99	-6.34		
Bi2O3	-1.44	0.01	*0.00*		
P2O5	-11.83	-8.71	-7.29		-5.05
UO2	-2.99	0.39	0.28		
Others	-2.51	-1.63	-1.68		

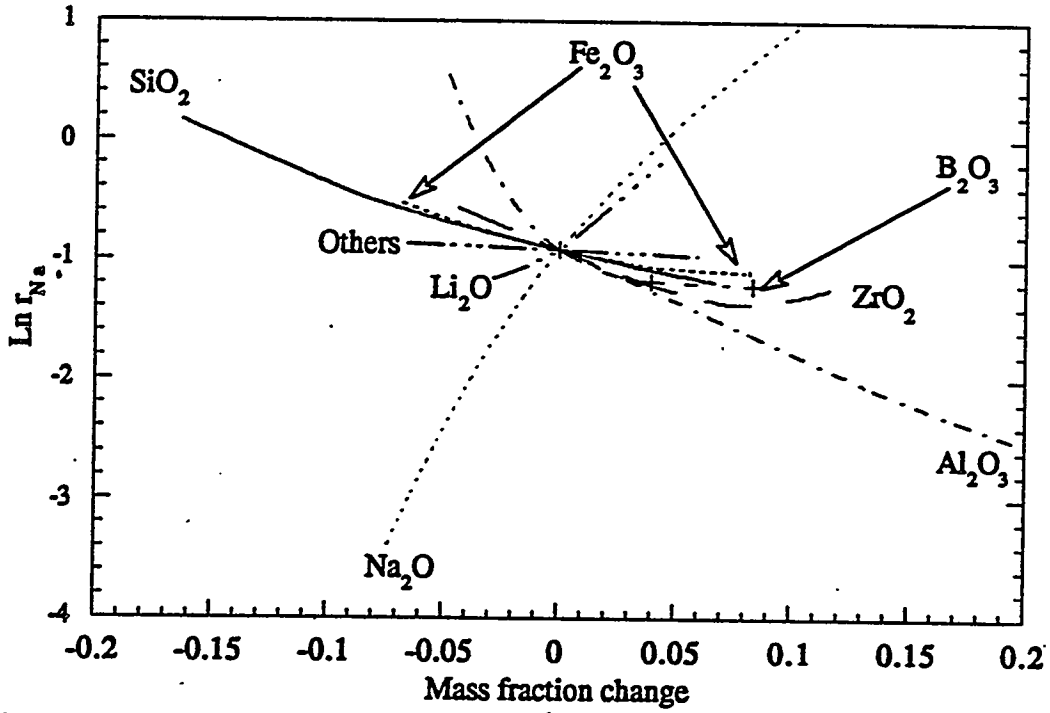

Figure 17. Normalized Na release as a function of component change from baseline glass.

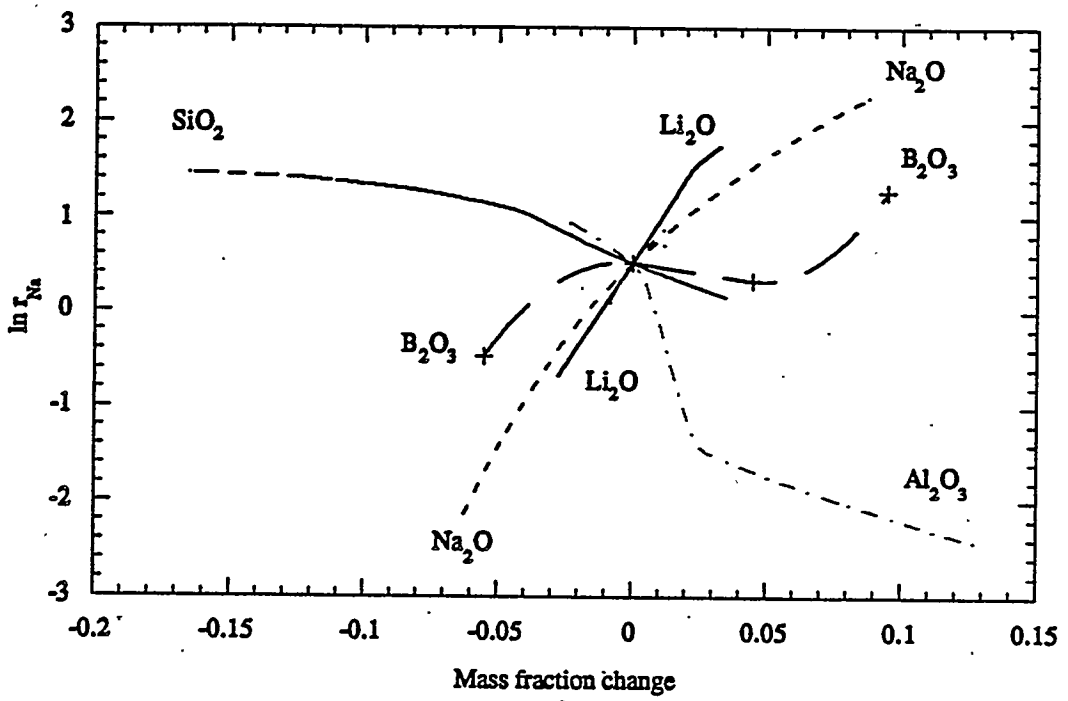

Figure 18. Normalized Na release as a function of component change from HW39-4 glass.

5.13 Canister Centerline Cooling Crystallinity and its Effect on PCT

The thermal history of a canister cooled glass has been a major concern in waste vitrification. In this complex process, part of the glass is quenched due to immediate contact with canister walls, while a portion of the glass located near the canister centerline is cooled slowly. Centerline cooling represents the lowest cooling rate which is typically experienced by glass in the canister, whereas quenching brackets the highest cooling rate. Hence, the thermal history of the glass in a canister falls in the range between quenched and centerline cooled. Cooled glass can also be reheated when it comes in contact with hot, freshly poured glass. This secondary phenomenon, which can affect crystallization, has not been addressed in the present study.

Heat treatment may affect chemical durability of glass. Mendel and McElroy (1972) have shown the durability of phosphate glasses to decrease by three orders of magnitude if heat treated at 620 - 650 °C for 24 hr or longer, but the effect was small when a boro-silicate glass received the same treatment. It was later shown that the decrease in durability was related to crystallization (Mendel, et al., 1977; Malow, et al., 1980). The effect of crystallization depends on thermal history plus the nature of crystalline phase present. Crystallization alters the surrounding glass composition, forms stresses, and may cause microcracking; all these may effect durability.

Durability of CCC glasses has been systematically measured previously in the CVS. Kim et al. (1995) showed a relationship between precipitation of certain crystalline phases and glass durability. The detrimental phases were nepheline, crystoballite, and eucriptite. The loss of durability was attributed to the change in residual glass composition. Crystoballite crystallization resulted in an additional loss of durability due to internal stresses. If no crystallization occurs, CCC treatment leads to a slight increase in durability as a result of structural relaxation and densification of the glass.

A simulated time/temperature history has been developed and verified for HLW glass melted at 1150°C by Lee (1989). The same cooling parameters have been applied to higher temperature melting HLW glasses (Langowski et al. 1994), see Figure 19.

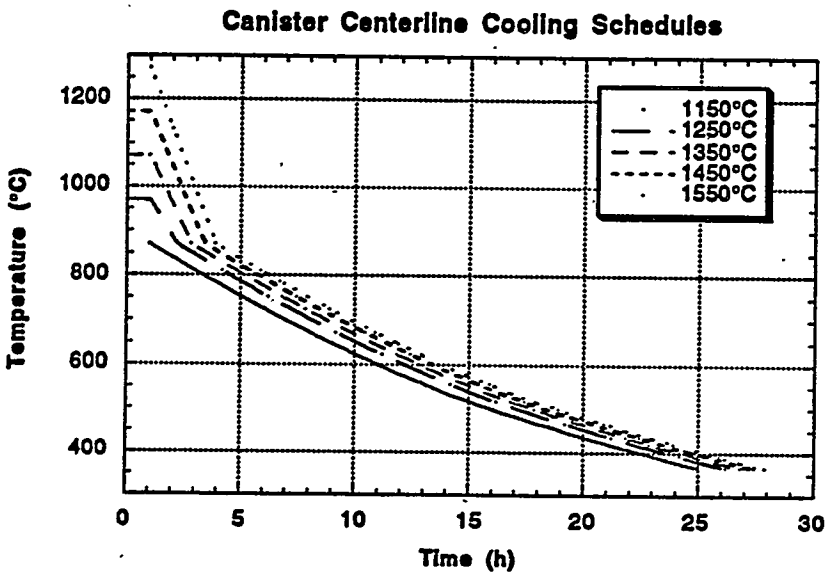

Figure 19. Simulated canister centerline cooling schedules for five starting temperatures.

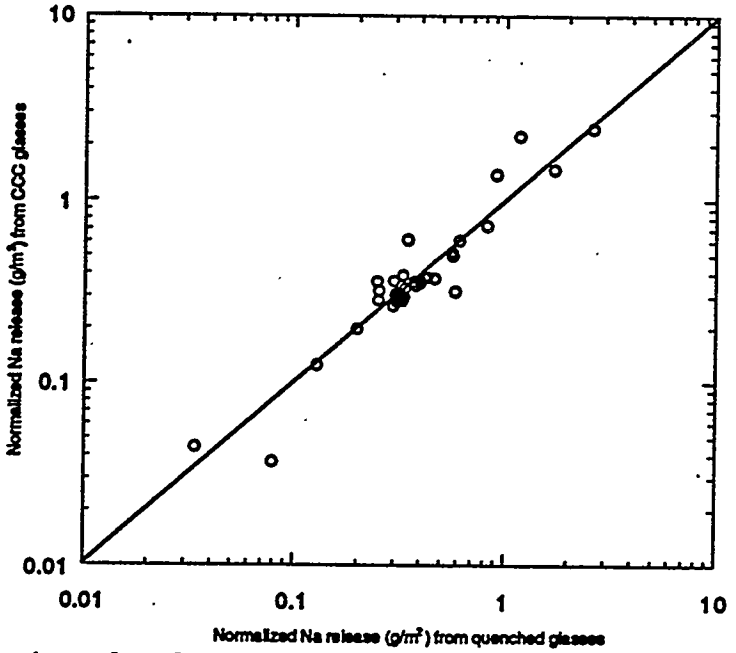

Figure 20. Comparison of r_{Na} from quenched and canister centerline cooled glass samples.

The crystallinity results for quenched and CCC glasses are listed in Section 10.4. The normalized Na release of CCC glasses are compared to those from quenched samples in Figures 6 to 16 and 20. Generally, the durability of CVS-III glasses was not substantially effected by CCC treatment. Even glasses with high crystallinity (up to nearly 100 vol%) showed little difference in r_{Na} between quenched and CCC samples. Glasses with no crystallinity became generally more durable after CCC treatment. Crystallization often resulted in a decrease in durability with some exceptions. A more complete investigation into the effects of crystallinity on glass durability has been accomplished for CVS-I and -II glasses (Kim et al., 1995).

6.0 Property Modelling

First- and second-order mixture models (Equation (3)) have been fitted to selected transformed glass properties. The coefficients in Tables X and XI were obtained by applying least squares regression to the whole set of CVS-III data including the low-temperature CVS internal standard glass (CVS3-26). First- and second-order models for normalized PCT release from quenched and CCC CVS glasses are reported by Piepel et al. (1995b) along with more thorough discussion.

Table X. First-order model coefficients for selected glass properties.

Coefficient	SiO_2	B_2O_3	Na_2O	Li_2O	Fe_2O_3	Al_2O_3	ZrO_2	Bi_2O_3	P_2O_5	UO_2	Others	R^2
A (w/ T_g)	-4.620	13.192	-6.654	2.087	-8.555	-11.175	-42.388	-7.185	-13.283		-11.166	0.912
B (w/ T_g)	16,311	-38,632	-6,026	-57,091	3,476	23,488	67,018	4,788	27,165		4,816	0.930
T_0 (w/ T_g)	358.3	1,856.7	429.7	1,040.4	659.7	586.6	-624.5	374.3	56.7		784.4	0.752
A (w/o T_g)	8.812	-22.281	-31.884	-41.916	-12.713	10.971	-11.214	-1.611	3.611	3.212	-37.452	0.708
B (w/o T_g)	-10,370	29,585	41,752	26,285	11,799	-19,054	-1,578	-5,855	-10,948	-4,286	63,075	0.598
T_0 (w/o T_g)	1,880.5	-1,962.1	-2,379.8	-3,879.1	248.9	2,985.1	2,216.0	801.7	1,863.3	2,227.2	-2,041.7	0.709
E_η	18.499	1.569	-40.848	-59.578	-28.860	-26.363	-54.808	-13.680	-10.127	-45.322	-71.467	0.444
F_η	-12,356	-19,434	41,656	19,039	38,179	58,380	99,701	15,231	27,434	66,616	101,084	0.394
$\ln \varepsilon_M$	-3.878	-2.256	8.148	8.187	2.011	3.051	4.533	1.337	3.130		0.471	0.741
E_ε	8.420	7.176	9.010	24.394	9.641	4.285	15.197	10.092	-1.154		5.385	0.467
F_ε	-11,100	-6,786	5,765	-3,073	-9,609	-5,703	-19,580	-10,419	6,116		-1,527	0.573

Table XI. Second-order model coefficients for selected glass properties.

	A w/ T_g	B w/ T_g	T_0 w/ T_g	A w/o T_g	B w/o T_g	T_0 w/o T_g	E_η	F_η	ln ε_M	E_ε	F_ε
SiO_2	-4.899	16,690	384.4	-2.262	434,210	-22,821.0	569.795	-817,857	-1.804	12.019	24,186
B_2O_3	11.933	-36,430	1,863.5	-43.246	-85,226	4,536.9	-211.573	291,987	1.547	10.586	-19,423
Na_2O	-7.219	-5,118	456.9	-45.074	-78,630	4,487.7	-214.818	295,845	11.125	11.784	-5,986
Li_2O	32.318	-104,776	1,072.7	-129.375	74,808	-8,754.2	-238.374	280,278	11.531	27.629	-15,065
Fe_2O_3	-9.363	4,844	676.6	38.345	-222,993	14,377.0	-223.719	322,887	5.387	26.233	-44,119
Al_2O_3	-11.878	24,679	-200.7	-4.937	-130,146	9,301.8	-203.868	317,733	6.075	-14.764	11,504
ZrO_2	-43.309	68,585	-604.2	-21.038	-132,882	9,726.1	-247.536	381,298	2.624	18.214	-31,559
Bi_2O_3	-8.645	6,278	380.9	-19.032	-181,576	6,954.1	-208.294	299,581	4.723	13.101	-22,219
P_2O_5	-37.139	84,975	-2,863.3	-17.783	-127,610	8,458.3	-226.526	343,617	7.292	2.350	-6,672
UO_2				10.531	-173,966	11,736.0	-226.904	331,927			
Others	-10.612	2,805	1,007.7	148.960	-466,297	26,051.0	-226.085	326,998	-9.475	-38.555	-16,158
$(SiO_2)^2$					-543,812	30,415.0	-741.229	1,083,012	9.029		-47,641
$(Li_2O)^2$	-406.501	643,531		919.751	-2,272,467	156,335.0					
$(Fe_2O_3)^2$				-612.256	1,008,976	-645,969.0				-76.698	125,654
$(Al_2O_3)^2$			4,112.0							86.416	-112,161
$(ZrO_2)^2$									30.714		
$(Bi_2O_3)^2$					443,148						
$(P_2O_5)^2$	268.887	-662,570	34,995.0								
(Others)^2				-796.641	1,642,843	-83,843.0			47.819	180.456	
R^2	0.945	0.957	0.878	0.865	0.883	0.895	0.705	0.676	0.818	0.732	0.802

7.0 Conclusions

- High temperature glasses for Hanford wastes are low in B_2O_3 and Li_2O. Their main flux component is Na_2O, the need for which can be fully covered from Hanford HLW. These glasses can be higher in refractory oxides (Al_2O_3, Fe_2O_3, ZrO_2, CeO_2, etc.) than low-temperature glasses without precipitation of crystalline phases in the melter.

- The T_M of HLW glasses can be decreased most effectively by Li_2O, followed by Na_2O and B_2O_3. However, the most effective component that decreases T_M and T_L simultaneously is Na_2O. SiO_2, Al_2O_3, and P_2O_5 increase T_M.

- SiO_2 addition increases the gap between T_M and T_L. Therefore, the addition of SiO_2 is desirable for increased waste loading. Although T_M increases with increasing SiO_2 content, Na_2O from Hanford HLW reduces the T_M without effecting the gap between T_M and T_L. Hence, the T_M of high-waste loaded glasses is moderate (approximately 1350°C).

- Electrical conductivity of high-temperature HLW glasses depends on the concentration of alkaline oxides. The supply of Na_2O from Hanford HLW is sufficient for molten glass to conduct electricity.

- Glass viscosity must be predicted accurately because it determines the T_M. VFT equation fitted to data augmented by low temperature viscosity (such as that at T_g) is adequate for viscosity/temperature correlation over a wide temperature range. First- or second-order coefficients for VFT parameters are sufficient to cover broad composition regions. However, these coefficients differ for low- and high-temperature glasses.

- Glass length is most increased by ZrO_2 and decreased by Li_2O. Hence, ZrO_2 makes HLW glass viscosity sensitive to temperature fluctuations, whereas Li_2O has an opposite effect.

- T_g for high-temperature HLW glasses is within 440 and 550°C. It is lowered by alkaline oxides and Bi_2O_3 and raised by Al_2O_3, ZrO_2, B_2O_3, Fe_2O_3, and SiO_2.

- Less common components may significantly affect glass properties. Bi_2O_3 decreases T_M, T_g, and T_L. P_2O_5 decreases T_M and T_L, exhibits and anomalous effect on T_g, and has a positive effect on glass durability. UO_2 decreases T_M, makes glass longer, and has little effect on durability. TiO_2 decreases T_M and increases durability. Cr_2O_3 increases durability.

- Significant differences were found between averaged and local values of component effects on glass durability. Also, glass components may affect high- and low-temperature glasses differently. For example, B_2O_3 increases durability of high-temperature glasses and decreases durability of low-temperature glasses. For other components, the trends are similar but the magnitudes of effects can be different. For example, SiO_2 and Li_2O component effects are significantly different in high- and low-temperature glasses.

- Al_2O_3 and B_2O_3 exhibit a remarkably nonlinear behavior in their effects on glass durability.

- Canister centerline cooling slightly increases glass durability except when a substantial fraction of glass is crystallized. The durability of a crystallized glass may decrease or, seldomly, increase. None of the high-temperature glasses tested in this study exhibited an unacceptable decrease in durability due to canister centerline cooling.

8.0 Recommendations

- A thorough statistically designed testing is needed to cover the full composition region of Hanford high-temperature HLW glasses. Such a study has never been performed. A test plan for this testing was written by Piepel et al. (1995).

- The composition region of low-temperature Hanford HLW glasses should be extended to include the high waste loading subregion. Previous studies (Hrma, Piepel, et al. 1994) focussed on glasses loaded with less than 30 wt% HLW, while waste loadings up to 65 wt% are achievable.

- Effects of key minor components, such as Cr_2O_3, NiO, CeO_2, and others (see Piepel et al. 1995) need a study to determine their effect on the maximum waste loading and glass

properties. This knowledge will reduce the likelihood of production failures, support pretreatment and blending studies, and provide data for glass formulation and melter design and operation.

- Studies that focus on high waste loading glasses are needed. These studies will involve T_L testing and modelling. Waste loading maximization will shorten production time and reduce storage space.

- Components and processes that can interfere with steady melting should be identified. A coldcap melting study is needed to avoid production interruptions.

9.0 References

BC Bunker. "Waste Glass Leaching: Chemistry and Kinetics," *Scientific Basis for Nuclear Waste Management X*, Materials Research Society, Pittsburgh, PA (1987).

BC Bunker. "Molecular Mechanisms for Corrosion of Silica and Silicate Glasses," *J. Non-Crystalline Solids*, Vol 179 (1994).

JJ DeYoreo and A Navrotsky, "Energetics of the Charge-Coupled Substitution $Si^{4+} \rightarrow Na^{+} + T^{3+}$ in Glasses $NaTO_2 \cdot SiO_2$ (T = Al, Fe, Ga, B)," J. Am. Ceram. Soc., vol 73 [7] pp 2068-72 (1990).

XD Feng, IL Pegg, A Barkatt, PB Mecedo, SJ Cucinell, and S Lai, "Correlation Between Composition Effects on Glass Durability and the Structural Role of the Constituent Oxides," Nuclear Technology, vol 85, pp334-45 (1989).

P Hrma and RJ Robertus, "Waste Glass Design Based on Property Composition Functions," Ceram. Eng. Sci. Proc. 14 [11-12] 187-203 (1993).

P Hrma, GF Piepel, MJ Schweiger, DE Smith, DS Kim, PE Redgate, JD Vienna, CA LoPresti, DB Simpson, DK Peeler, and MH Langowski, "Property/Composition Relationships for Hanford High-Level Waste Glasses Melting at 1150°C," PNL-10359, Vol. 1 and 2, Pacific Northwest Laboratory, Richland, Washington (1994).

P Hrma, GF Piepel, PE Redgate, DE Smith, MJ Schweiger, JD Vienna, and DS Kim, "Prediction of Processing Properties for Nuclear Waste Glasses," Ceram. Trans. (1995).

PR Hrma and JD Vienna, "Maximization of Hanford Waste Loading, Investigation Plan," PVTD-C95-02.01R, Pacific Northwest Laboratory, Richland, Washington (1995)

DS Kim. "PNL Vitrification Technology Development Project, Evaluation and Recommendation of Candidate Glass Systems for LLW Vitrification: Glass Formulation Technical Status Report," PVTD-C94-02.01C, Pacific Northwest Laboratory, Richland, Washington (1994).

KS Kim and P Hrma, "Models for Liquidus Temperature of Nuclear Waste Glasses," Ceram. Trans. 45, 327-337 (1994).

DS Kim and P Hrma, "Development of High-Waste Loaded High-Level Nuclear Waste Glasses for High-Temperature Melter," Ceram. Trans. 45, 39-47 (1994).

KS Kim and P Hrma, "Durability of Silicate Glasses with High Level of Sodium for LLW vitrification," Emerging Technologies in Hazardous Waste Management (1995).

KS Kim, DK Peeler, and P Hrma, "Effects of Crystallization on the Chemical Durability of Nuclear Waste Glasses," Ceram. Trans. in press (1995).

WC LaCourse and HJ Stevens. "Properties of Silica Glasses Containing Small Amounts of B_2O_3," *Borate Glasses: Structure, Properties, Applications*, eds. LD Pye, VD Frechette, and NJ Kreidl, Plenum Press, NY (1977).

SL Lambert and DS Kim, "Tank Waste Remediation System High-Level Waste Feed Processability Assessment Report," WHC-SP-1143, Westinghouse Hanford Company, Richland, WA (1994).

MH Langowski, JD Vienna, PR Hrma, and GF Piepel, "The Glass Composition Envelope Definition Fiscal Year 1994 Test Plan," PVTD-C94-03.01E Rev. 1 Pacific Northwest Laboratory, Richland, Washington (1994).

H Li, MH Langowski, PR Hrma, MJ Schweiger, JD Vienna, and DE Smith, "Minor Component Study for Simulated High-Level Waste Glasses," PVTD-T3C-95-125, Pacific Northwest Laboratory, Richland, Washington (1995).

H Li, "Letter Report — Minor Component Study for Low-Level Radioactive Waste Glasses," PVTD-C95-02.01B Pacific Northwest Laboratory, Richland, Washington (1995).

L Lee, "Thermal Analysis of DWPF Canister During Poring and Cooldown," DPST-89-269, Westinghouse Savannah River Co., Aiken, SC (1989).

G Malow, JAC Marples and C Sombret, "Thermal and Radiation Effects on Properties of High Level Waste Products." Radioactive Waste Management and Disposal. R. Simon and s. Orlowski, editors, Harwood Academic Publishers, Chur, Switzerland (1980).

JE Mendel and JL McElroy, Waste Solidification Program Volume 10. Evaluation of Solidified Waste Products. BNWL - 1666, Pacific Northwest Laboratory, Richland, Washington, pp. 5.7 - 5.9 (1972).

Mendel, J. E., W. A. Ross, F. P. Roberts, Y. B. Katayama, J. H. Westsik, Jr., R. P. Turcotte, J. W. Wald and D. J. Bradley. 1977. Annual Report on the Characteristics of High-Level Waste Glasses. BNWL - 2252, Pacific Northwest Laboratory, Richland, Washington.

RA Merrill and CC Chapman, "Preliminary Estimates of Cost Savings for Defense High-Level Waste Vitrification Options," Proceedings, 1993 Int. Conf. on Nucl. Waste Mgt and Env. Rem., Vol 3, pp 799-807 (1993).

DK Peeler and P Hrma, "Predicting Liquid Immiscibility in Multicomponent Nuclear Waste Glasses," Ceram. Trans. 45, 219-229 (1994).

GF Piepel, JD Vienna, PE Redgate, and H Li, "Glass Composition Envelope Definition FY95-96 Test Plan for High-Temperature Melter Glass Formulation and Testing," T3C-95-133, Pacific Northwest Laboratory, Richland, WA (1995).

GF Piepel, SA Hartley, and PE Redgate, "Updated Durability/Composition Relationships for Hanford High-Level Waste Glasses," T3C-95-126, Rev. 0, Pacific Northwest Laboratory, Richland, WA (1995b).

HD Schreiber and GB Balazs, "The Chemistry of Uranium in Boro-silicate Glasses. Part 1. Simple Base Compositions Relevant to the Immobilization of Nuclear Waste," Phys. and Chem. of Glass. Vol 23, [5] pp 139-46 (1982).

HD Schreiber, BK Kochanowski, and CW Schreiber, "Compositional Dependance of Redox Equilibria in Sodium Silicate Glasses," *J. Non-Crystalline Solids*, Vol 177 (1994).

M Volf. "Chemical Approach to Glass," Elsevier Press, NY (1984).

10.0 Raw Data

10.1 All-Blend Waste Simulant Composition

All Blend Waste Simulant	
SiO2	0.1237
B2O3	0.0009
Na2O	0.2467
Li2O	0.0000
CaO	0.0252
MgO	0.0009
Fe2O3	0.1360
Al2O3	0.0974
ZrO2	0.0875
Bi2O3	0.0275
P2O5	0.0159
Others	0.2383
Total	1.0000

Others For All Blend Waste	
CdO	0.1124
CeO2	3.3785
Cr2O3	1.0587
F	0.6791
K2O	0.2625
La2O3	0.5290
MnO2	2.2451
MoO3	0.0910
Nd2O3	12.0422
NiO	2.8070
SO3	0.4083
WO3	0.2149
Total	23.8287

10.2 Viscosity Temperature Table

#	T(C)	1/T (K-1)	Vis (Pa.s)	ln Visc
1	1095	0.0007	76.0791	4.3318
1	1145	0.0007	40.6836	3.7058
1	1194	0.0007	23.1979	3.1441
1	1244	0.0007	14.1354	2.6487
1	1245	0.0007	14.3568	2.6642
1	1294	0.0006	8.8702	2.1827
1	1294	0.0006	9.0916	2.2073
1	1295	0.0006	9.1074	2.2091
1	1344	0.0006	5.9372	1.7812
1	1395	0.0006	4.0161	1.3903
2	1194	0.0007	74.0607	4.3049
2	1245	0.0007	41.3039	3.7210
2	1294	0.0006	23.4347	3.1542
2	1344	0.0006	14.7855	2.6936
2	1344	0.0006	15.0087	2.7086
2	1394	0.0006	8.8410	2.1794
2	1395	0.0006	10.2664	2.3289
2	1395	0.0006	10.4636	2.3479
2	1445	0.0006	7.2353	1.9790
2	1497	0.0006	5.4573	1.6969
3	1000	0.0008	71.0640	4.2636
3	1100	0.0007	16.7226	2.8168
3	1150	0.0007	9.9264	2.2952
3	1199	0.0007	5.6753	1.7361
3	1200	0.0007	5.8163	1.7607
3	1235	0.0007	4.0115	1.3892
3	1235	0.0007	4.0538	1.3996
3	1235	0.0007	3.9480	1.3732
3	1300	0.0006	2.2222	0.7985
3	1350	0.0006	1.5454	0.4353
4	1044	0.0008	16.6764	2.8140
4	1094	0.0007	10.9034	2.3891
4	1143	0.0007	6.1885	1.8227
4	1144	0.0007	5.8498	1.7664
4	1193	0.0007	3.3329	1.2038
4	1194	0.0007	3.5869	1.2773
4	1194	0.0007	3.1712	1.1541
4	1244	0.0007	1.9735	0.6798
5	1051	0.0008	188.3760	5.2384
5	1126	0.0007	21.0372	3.0463
5	1126	0.0007	21.2628	3.0570
5	1126	0.0007	7.8678	2.0628
5	1200	0.0007	1.9655	0.6758
6	1043	0.0008	35.0371	3.5564

#	T(C)	1/T (K-1)	Vis (Pa.s)	ln Visc
6	1094	0.0007	19.4265	2.9666
6	1144	0.0007	11.7677	2.4654
6	1195	0.0007	7.2584	1.9822
6	1244	0.0007	4.7183	1.5515
6	1245	0.0007	4.6799	1.5433
6	1294	0.0006	3.1712	1.1541
6	1294	0.0006	3.2097	1.1662
6	1295	0.0006	3.2328	1.1733
6	1344	0.0006	2.2353	0.8044
7	1093	0.0007	37.8857	3.6346
7	1144	0.0007	21.2990	3.0587
7	1194	0.0007	12.6776	2.5398
7	1244	0.0007	7.8553	2.0612
7	1244	0.0007	7.9159	2.0689
7	1294	0.0006	5.1494	1.6389
7	1294	0.0006	5.3187	1.6712
7	1295	0.0006	5.3803	1.6827
7	1344	0.0006	3.6331	1.2901
7	1395	0.0006	2.5708	0.9442
8	992	0.0008	40.2785	3.6958
8	1043	0.0008	21.1234	3.0504
8	1094	0.0007	12.1772	2.4996
8	1144	0.0007	7.2199	1.9768
8	1194	0.0007	4.4797	1.4996
8	1194	0.0007	4.4566	1.4944
8	1243	0.0007	2.8910	1.0616
8	1244	0.0007	2.9342	1.0764
8	1245	0.0007	2.9619	1.0858
8	1294	0.0006	2.0043	0.6953
9	1244	0.0007	60.7857	4.1074
9	1294	0.0006	34.4104	3.5384
9	1344	0.0006	20.3042	3.0108
9	1394	0.0006	12.9354	2.5600
9	1394	0.0006	13.4207	2.5968
9	1444	0.0006	8.4467	2.1338
9	1444	0.0006	8.8713	2.1828
9	1445	0.0006	8.9926	2.1964
9	1495	0.0006	6.1577	1.8177
9	1547	0.0005	4.7568	1.5596
10	949	0.0008	65.5650	4.1830
10	1000	0.0008	30.8508	3.4292
10	1100	0.0007	8.7279	2.1665
10	1149	0.0007	5.1042	1.6301
10	1199	0.0007	3.1373	1.1433

#	T(C)	1/T (K-1)	Vis (Pa.s)	ln Visc
10	1199	0.0007	3.2430	1.1765
10	1249	0.0007	2.1347	0.7583
10	1249	0.0007	2.1770	0.7780
10	1249	0.0007	2.2334	0.8035
10	1299	0.0006	1.5143	0.4150
11	992	0.0008	93.9034	4.5423
11	1042	0.0008	46.1465	3.8318
11	1094	0.0007	24.9268	3.2159
11	1143	0.0007	14.3002	2.6603
11	1193	0.0007	8.5528	2.1463
11	1193	0.0007	8.6135	2.1533
11	1243	0.0007	5.5342	1.7110
11	1243	0.0007	5.6574	1.7330
11	1244	0.0007	5.7113	1.7424
11	1294	0.0006	3.7254	1.3152
11	1344	0.0006	2.5585	0.9394
12	1245	0.0007	92.0868	4.5227
12	1294	0.0006	49.1659	3.8952
12	1344	0.0006	27.7062	3.3217
12	1394	0.0006	16.5886	2.8087
12	1394	0.0006	17.2323	2.8468
12	1444	0.0006	10.6607	2.3666
12	1445	0.0006	11.2218	2.4179
12	1446	0.0006	11.1157	2.4084
12	1496	0.0006	7.9159	2.0689
12	1547	0.0005	5.5112	1.7068
13	1093	0.0007	42.9927	3.7610
13	1144	0.0007	22.9662	3.1340
13	1194	0.0007	18.4786	2.9166
13	1244	0.0007	10.3769	2.3396
13	1244	0.0007	10.6931	2.3696
13	1294	0.0006	5.8297	1.7630
13	1294	0.0006	5.9205	1.7784
13	1295	0.0006	5.1114	1.6315
13	1344	0.0006	3.5689	1.2723
13	1396	0.0006	2.2744	0.8217
14	1093	0.0007	59.3883	4.0841
14	1144	0.0007	30.6504	3.4226
14	1195	0.0007	18.6366	2.9251
14	1244	0.0007	11.3583	2.4299
14	1245	0.0007	10.9792	2.3960
14	1294	0.0006	7.0121	1.9476
14	1295	0.0006	6.7658	1.9119
14	1295	0.0006	7.0583	1.9542

#	T(C)	1/T (K-1)	Vis (Pa.s)	ln Visc
14	1345	0.0006	4.5182	1.5081
14	1395	0.0006	3.1635	1.1517
15	1143	0.0007	66.7944	4.2016
15	1194	0.0007	36.8032	3.6056
15	1244	0.0007	21.6208	3.0737
15	1294	0.0006	13.7240	2.6191
15	1294	0.0006	13.8908	2.6312
15	1343	0.0006	8.6742	2.1603
15	1344	0.0006	8.9320	2.1896
15	1345	0.0006	8.9471	2.1913
15	1394	0.0006	6.1038	1.8089
15	1445	0.0006	4.1334	1.4191
16	1244	0.0007	120.4377	4.7911
16	1295	0.0006	45.9162	3.8268
16	1345	0.0006	38.7508	3.6572
16	1395	0.0006	18.5079	2.9182
16	1395	0.0006	20.4731	3.0191
16	1445	0.0006	9.5335	2.2548
16	1445	0.0006	10.1660	2.3190
16	1446	0.0006	8.7654	2.1708
16	1496	0.0006	5.6558	1.7327
16	1547	0.0005	4.1209	1.4161
17	1245	0.0007	60.5062	4.1027
17	1295	0.0006	32.0746	3.4681
17	1345	0.0006	19.9239	2.9919
17	1395	0.0006	12.0559	2.4896
17	1395	0.0006	12.3743	2.5156
17	1444	0.0006	7.5355	2.0196
17	1445	0.0006	7.4913	2.0137
17	1446	0.0006	7.4307	2.0056
17	1496	0.0006	5.0570	1.6208
17	1547	0.0005	4.2873	1.4557
18	1194	0.0007	61.9796	4.1268
18	1245	0.0007	33.9929	3.5262
18	1294	0.0006	19.2999	2.9601
18	1344	0.0006	12.0335	2.4877
18	1344	0.0006	12.2896	2.5088
18	1394	0.0006	7.6358	2.0328
18	1395	0.0006	7.8165	2.0562
18	1396	0.0006	8.0123	2.0810
18	1446	0.0006	5.2551	1.6592
18	1496	0.0006	4.0831	1.4069
19	1095	0.0007	42.1135	3.7404
19	1145	0.0007	23.3818	3.1520

#	T(C)	1/T (K-1)	Vis (Pa.s)	ln Visc
19	1194	0.0007	13.6049	2.6104
19	1244	0.0007	8.5366	2.1444
19	1244	0.0007	8.6131	2.1533
19	1294	0.0006	5.5339	1.7109
19	1294	0.0006	5.6508	1.7318
19	1295	0.0006	5.6451	1.7308
19	1345	0.0006	3.8140	1.3387
19	1395	0.0006	2.6561	0.9769
20	1194	0.0007	94.2372	4.5458
20	1245	0.0007	35.8273	3.5787
20	1295	0.0006	80.0100	4.3822
20	1345	0.0006	24.3155	3.1911
20	1345	0.0006	23.2009	3.1442
20	1395	0.0006	11.6871	2.4585
20	1395	0.0006	10.3467	2.3367
20	1396	0.0006	5.7466	1.7486
20	1446	0.0006	5.1643	1.6418
20	1496	0.0006	2.3818	0.8679
21	1144	0.0007	73.1078	4.2919
21	1195	0.0007	32.1586	3.4707
21	1245	0.0007	21.5584	3.0708
21	1294	0.0006	12.4402	2.5209
21	1295	0.0006	11.8829	2.4751
21	1344	0.0006	6.7220	1.9054
21	1345	0.0006	7.1756	1.9707
21	1346	0.0006	6.1095	1.8098
21	1395	0.0006	4.1889	1.4324
21	1446	0.0006	2.5708	0.9442
22	1094	0.0007	106.8989	4.6719
22	1144	0.0007	51.7866	3.9471
22	1195	0.0007	27.5892	3.3174
22	1244	0.0007	15.0965	2.7145
22	1294	0.0006	9.2201	2.2214
22	1295	0.0006	9.4172	2.2425
22	1344	0.0006	5.9037	1.7756
22	1345	0.0006	6.0961	1.8077
22	1345	0.0006	6.1269	1.8127
22	1395	0.0006	3.9640	1.3773
22	1446	0.0006	2.7156	0.9990
23	1144	0.0007	30.2516	3.4095
23	1194	0.0007	18.5781	2.9220
23	1244	0.0007	11.6464	2.4550
23	1294	0.0006	7.5975	2.0278
23	1294	0.0006	7.7946	2.0534

#	T(C)	1/T (K-1)	Vis (Pa.s)	ln Visc
23	1344	0.0006	5.2110	1.6508
23	1345	0.0006	5.4496	1.6955
23	1345	0.0006	5.5727	1.7179
23	1396	0.0006	3.8101	1.3377
23	1446	0.0006	2.7525	1.0125
24	1093	0.0007	54.8630	4.0048
24	1144	0.0007	29.0552	3.3692
24	1194	0.0007	17.3785	2.8552
24	1244	0.0007	10.3726	2.3392
24	1244	0.0007	10.6152	2.3623
24	1294	0.0006	6.3655	1.8509
24	1295	0.0006	6.5503	1.8795
24	1295	0.0006	6.3732	1.8521
24	1345	0.0006	4.1257	1.4172
24	1396	0.0006	2.7741	1.0203
25	1193	0.0007	33.2710	3.5047
25	1244	0.0007	19.9239	2.9919
25	1293	0.0006	12.7383	2.5446
25	1343	0.0006	8.1889	2.1028
25	1344	0.0006	8.2799	2.1138
25	1393	0.0006	5.6497	1.7316
25	1394	0.0006	5.7267	1.7451
25	1394	0.0006	5.6728	1.7357
25	1444	0.0006	3.9025	1.3616
25	1495	0.0006	2.9126	1.0690
27	1094	0.0007	43.4119	3.7707
27	1144	0.0007	23.0251	3.1366
27	1195	0.0007	16.4131	2.7981
27	1244	0.0007	9.7660	2.2789
27	1245	0.0007	9.4476	2.2458
27	1295	0.0006	5.5189	1.7082
27	1295	0.0006	5.7190	1.7438
27	1296	0.0006	5.2648	1.6611
27	1345	0.0006	3.5946	1.2794
27	1396	0.0006	2.3676	0.8619
28	1093	0.0007	63.9517	4.1581
28	1144	0.0007	33.5343	3.5126
28	1194	0.0007	19.1532	2.9525
28	1244	0.0007	11.9281	2.4789
28	1244	0.0007	12.0335	2.4877
28	1293	0.0006	7.6358	2.0328
28	1294	0.0006	7.6509	2.0348
28	1295	0.0006	7.6057	2.0289
28	1344	0.0006	5.2702	1.6621

#	T(C)	1/T (K-1)	Vis (Pa.s)	ln Visc
28	1395	0.0006	3.6597	1.2974
29	1093	0.0007	55.6613	4.0193
29	1144	0.0007	29.9803	3.4005
29	1194	0.0007	17.1000	2.8391
29	1244	0.0007	10.6329	2.3640
29	1244	0.0007	10.7986	2.3794
29	1294	0.0006	6.9034	1.9320
29	1294	0.0006	6.9942	1.9451
29	1295	0.0006	6.9488	1.9386
29	1345	0.0006	4.8543	1.5799
29	1395	0.0006	3.2665	1.1837
30	1043	0.0008	76.0659	4.3316
30	1093	0.0007	38.3495	3.6467
30	1143	0.0007	20.9717	3.0432
30	1193	0.0007	12.6510	2.5377
30	1193	0.0007	12.7866	2.5484
30	1243	0.0007	7.8165	2.0562
30	1243	0.0007	7.9069	2.0677
30	1245	0.0007	7.8617	2.0620
30	1294	0.0006	5.1190	1.6330
30	1344	0.0006	3.7201	1.3138
31	993	0.0008	110.8590	4.7083
31	1043	0.0008	52.2792	3.9566
31	1093	0.0007	27.4246	3.3114
31	1142	0.0007	15.3695	2.7324
31	1143	0.0007	15.1348	2.7170
31	1192	0.0007	9.2624	2.2260
31	1193	0.0007	9.1569	2.2145
31	1194	0.0007	9.2774	2.2276
31	1243	0.0007	5.8902	1.7733
31	1294	0.0006	3.8638	1.3517
32	1160	0.0007	45.2097	3.8113
32	1241	0.0007	17.3786	2.8552
32	1289	0.0006	10.9996	2.3979
32	1289	0.0006	11.0338	2.4010
32	1337	0.0006	7.3502	1.9947
32	1338	0.0006	7.4016	2.0017
32	1338	0.0006	7.4701	2.0109
32	1424	0.0006	3.8293	1.3427
33	1162	0.0007	48.4700	3.8809
33	1234	0.0007	21.1323	3.0508
33	1281	0.0006	13.0213	2.5666
33	1281	0.0006	13.4839	2.6015
33	1329	0.0006	8.7722	2.1716

#	T(C)	1/T (K-1)	Vis (Pa.s)	ln Visc
33	1329	0.0006	9.1663	2.2155
33	1330	0.0006	9.2862	2.2285
33	1401	0.0006	5.2342	1.6552
34	1160	0.0007	56.8020	4.0396
34	1243	0.0007	18.9426	2.9414
34	1289	0.0006	11.9933	2.4843
34	1290	0.0006	11.9248	2.4786
34	1336	0.0006	7.6843	2.0392
34	1337	0.0006	7.9670	2.0753
34	1338	0.0006	9.2520	2.2248
34	1425	0.0006	4.5061	1.5054
35	1136.5	0.0007	60.7948	4.1075
35	1242	0.0007	16.1867	2.7842
35	1289	0.0006	10.3200	2.3341
35	1289	0.0006	10.3571	2.3377
35	1336	0.0006	6.8619	1.9260
35	1337	0.0006	6.8048	1.9176
35	1338	0.0006	6.9190	1.9343
35	1424	0.0006	3.8087	1.3373
36	1136.5	0.0007	94.1288	4.5447
36	1243	0.0007	15.1287	2.7166
36	1289	0.0006	9.7488	2.2771
36	1290	0.0006	9.6632	2.2683
36	1336	0.0006	6.4078	1.8575
36	1338	0.0006	6.3479	1.8481
36	1339	0.0006	6.3564	1.8495
36	1424	0.0006	3.6494	1.2946
37	1144	0.0007	48.6678	3.8850
37	1194	0.0007	27.4832	3.3136
37	1244	0.0007	15.5748	2.7457
37	1294	0.0006	10.0606	2.3086
37	1295	0.0006	9.8497	2.2874
37	1344	0.0006	6.3137	1.8427
37	1345	0.0006	6.6237	1.8906
37	1346	0.0006	6.6615	1.8963
37	1396	0.0006	4.4158	1.4852
37	1446	0.0006	3.0774	1.1241
38	1144	0.0007	54.8587	4.0048
38	1194	0.0007	30.5535	3.4195
38	1244	0.0007	17.3640	2.8544
38	1294	0.0006	11.1299	2.4096
38	1295	0.0006	10.9040	2.3891
38	1344	0.0006	7.0395	1.9515
38	1345	0.0006	7.3117	1.9895

#	T(C)	1/T (K-1)	Vis (Pa.s)	ln Visc
38	1346	0.0006	7.3269	1.9915
38	1396	0.0006	4.8619	1.5814
38	1446	0.0006	3.3421	1.2066
39	1144	0.0007	66.2050	4.1928
39	1194	0.0007	35.4260	3.5674
39	1244	0.0007	20.0920	3.0003
39	1294	0.0006	12.4400	2.5209
39	1294	0.0006	12.6360	2.5365
39	1344	0.0006	7.9220	2.0696
39	1344	0.0006	8.0880	2.0904
39	1345	0.0006	8.0270	2.0828
39	1396	0.0006	5.4590	1.6973
39	1446	0.0006	4.0000	1.3863
40	1194	0.0007	42.0180	3.7381
40	1245	0.0007	23.0540	3.1378
40	1295	0.0006	14.0670	2.6438
40	1295	0.0006	14.1720	2.6513
40	1344	0.0006	8.7200	2.1656
40	1345	0.0006	8.9160	2.1878
40	1346	0.0006	8.9910	2.1962
40	1396	0.0006	5.9810	1.7886
40	1447	0.0006	4.0230	1.3920

10.3 Electrical Conductivity Temperature Table

#	Glass	T (°C)	EC 100	EC 1000	EC 10000	EC 100000
1	CVS3-1	1446	58.839	58.635	61.227	61.598
1	CVS3-1	1347	42.299	45.549	47.137	47.371
1	CVS3-1	1248	30.185	33.709	34.275	34.451
1	CVS3-1	1148	21.193	23.077	23.740	23.909
2	CVS3-2	1498	41.130	49.205	50.125	49.991
2	CVS3-2	1397	31.511	31.728	32.265	32.287
2	CVS3-2	1297	22.372	23.928	24.481	24.586
2	CVS3-2	1197	15.610	17.275	17.681	17.712
3	CVS3-3	1345	66.047	67.954	70.228	70.297
3	CVS3-3	1247	46.297	51.069	52.301	52.305
3	CVS3-3	1148	33.031	36.117	37.079	37.101
3	CVS3-3	1048	21.231	23.652	24.140	24.215
4	CVS3-4	1245	58.410	63.098	64.412	64.249
4	CVS3-4	1147	42.591	46.130	47.640	47.606
4	CVS3-4	1048	28.218	31.369	32.066	32.233
4	CVS3-4	949	16.960	18.962	19.712	19.850
5	CVS3-5	1196	58.745	65.783	67.860	67.663
5	CVS3-5	1147	50.372	56.207	58.342	58.308
5	CVS3-5	1098	42.255	47.415	49.334	49.375
5	CVS3-5	1048	34.327	39.007	40.528	40.713
6	CVS3-6	1346	38.332	40.851	42.264	42.084
6	CVS3-6	1248	27.857	30.335	31.508	31.593
6	CVS3-6	1148	19.661	21.552	22.052	22.033
6	CVS3-6	1048	12.627	13.659	14.046	14.049
7	CVS3-7	1396	42.199	48.591	49.098	49.110
7	CVS3-7	1297	33.535	36.772	37.711	37.917
7	CVS3-7	1198	23.825	27.595	27.219	27.355
7	CVS3-7	1098	16.085	17.790	18.436	18.305
8	CVS3-8	1296	74.159	91.831	98.824	97.881
8	CVS3-8	1197	58.460	72.097	77.729	77.447
8	CVS3-8	1098	42.922	54.208	57.539	57.403
8	CVS3-8	998	29.715	37.302	39.673	39.739
9	CVS3-9	1549	36.134	36.616	37.287	37.184
9	CVS3-9	1448	30.280	25.757	26.194	26.166
9	CVS3-9	1347	18.237	18.815	19.138	19.146
9	CVS3-9	1247	12.970	13.410	13.555	13.587
10	CVS3-10	1295	75.783	85.833	88.874	88.510
10	CVS3-10	1197	55.733	63.102	65.943	65.814
10	CVS3-10	1098	38.889	44.463	46.073	46.073
10	CVS3-10	999	24.675	28.162	29.379	29.433
11	CVS3-11	1346	59.163	65.550	67.329	67.231
11	CVS3-11	1247	45.767	50.846	52.210	52.299
11	CVS3-11	1147	32.743	36.656	37.552	37.655
11	CVS3-11	1047	21.568	24.101	24.782	24.842

#	Glass	T (°C)	EC 100	EC 1000	EC 10000	EC 100000
12	CVS3-12	1549	39.250	41.443	41.960	41.961
12	CVS3-12	1448	26.587	31.942	32.135	32.180
12	CVS3-12	1348	22.565	24.267	24.711	24.785
12	CVS3-12	1248	17.189	18.099	18.482	18.495
13	CVS3-13	1397	45.722	49.360	49.983	49.874
13	CVS3-13	1299	37.091	37.974	38.401	38.367
13	CVS3-13	1199	26.304	27.687	27.854	27.878
13	CVS3-13	1099	17.827	18.596	18.707	18.751
14	CVS3-14	1397	47.030	51.649	52.996	53.327
14	CVS3-14	1298	35.745	39.397	40.317	40.495
14	CVS3-14	1198	25.613	28.398	28.806	28.974
14	CVS3-14	1098	17.243	18.624	19.169	19.224
15	CVS3-15	1447	46.878	53.877	58.238	57.528
15	CVS3-15	1347	35.415	43.002	46.493	45.963
15	CVS3-15	1248	26.957	32.986	34.870	34.589
15	CVS3-15	1147	19.469	23.367	24.528	24.487
16	CVS3-16	1551	47.101	43.811	43.544	43.757
16	CVS3-16	1451	31.869	32.096	32.496	32.558
16	CVS3-16	1350	23.489	24.413	24.700	24.780
16	CVS3-16	1250	16.559	17.643	18.123	18.306
17	CVS3-17	1498	36.839	45.005	45.895	45.823
17	CVS3-17	1398	33.266	35.953	36.566	36.587
17	CVS3-17	1298	25.433	27.077	27.734	27.821
17	CVS3-17	1198	17.684	19.459	20.068	20.155
18	CVS3-18	1498	48.170	54.964	56.412	56.082
18	CVS3-18	1398	37.375	42.653	43.713	43.489
18	CVS3-18	1298	28.573	31.810	32.645	32.547
18	CVS3-18	1198	20.086	22.703	23.353	23.342
19	CVS3-19	1446	56.386	93.303	122.322	132.552
19	CVS3-19	1347	48.658	67.157	81.274	86.044
19	CVS3-19	1248	35.484	46.327	52.873	54.838
19	CVS3-19	1148	25.055	30.991	33.935	34.724
20	CVS3-20	1499	52.069	66.608	68.290	68.578
20	CVS3-20	1399	39.319	48.100	49.060	49.425
20	CVS3-20	1299	30.591	34.688	35.693	35.948
20	CVS3-20	1200	21.441	24.241	24.716	24.834
21	CVS3-21	1448	47.818	63.684	70.264	64.544
21	CVS3-21	1349	35.481	46.785	50.282	47.408
21	CVS3-21	1250	26.518	32.324	34.103	32.837
21	CVS3-21	1149	17.755	20.935	21.986	21.483
22	CVS3-22	1446	37.442	41.619	43.229	42.662
22	CVS3-22	1347	28.045	31.814	32.819	32.560
22	CVS3-22	1247	20.747	22.952	23.766	23.627
22	CVS3-22	1147	14.154	15.607	16.089	16.067

#	Glass	T (°C)	EC 100	EC 1000	EC 10000	EC 100000
23	CVS3-23	1447	52.988	63.049	64.761	65.078
23	CVS3-23	1348	46.321	50.631	52.104	52.389
23	CVS3-23	1248	34.649	38.432	39.595	39.739
23	CVS3-23	1148	24.733	27.238	28.139	28.237
24	CVS3-24	1396	44.204	46.842	47.848	47.862
24	CVS3-24	1298	32.963	35.725	36.523	36.555
24	CVS3-24	1198	23.744	25.609	26.242	26.244
24	CVS3-24	1098	15.559	17.089	17.416	17.486
25	CVS3-25	1497	53.918	81.934	115.024	103.001
25	CVS3-25	1397	44.458	63.409	81.983	76.003
25	CVS3-25	1297	35.335	46.507	56.852	54.108
25	CVS3-25	1197	26.113	33.046	38.365	37.038
27	CVS3-27	1397	48.228	49.461	50.689	50.595
27	CVS3-27	1298	36.256	38.009	38.619	38.542
27	CVS3-27	1198	26.203	27.261	27.786	27.725
27	CVS3-27	1098	17.379	18.310	18.501	18.517
28	CVS3-28	1396	44.340	50.104	51.912	51.801
28	CVS3-28	1297	32.767	36.822	38.062	38.082
28	CVS3-28	1198	23.812	26.269	27.117	27.219
28	CVS3-28	1098	15.812	17.591	18.110	18.148
29	CVS3-29	1396	44.562	47.509	48.314	48.609
29	CVS3-29	1298	34.557	36.467	37.218	37.351
29	CVS3-29	1198	25.052	26.601	27.320	27.419
29	CVS3-29	1098	16.678	18.003	18.376	18.401
30	CVS3-30	1346	38.949	42.141	43.419	43.408
30	CVS3-30	1247	29.131	31.766	32.343	32.478
30	CVS3-30	1148	20.358	22.068	22.528	22.523
30	CVS3-30	1048	12.967	14.037	14.308	14.321
31	CVS3-31	1296	33.686	37.293	38.323	38.351
31	CVS3-31	1198	24.414	26.933	27.417	27.521
31	CVS3-31	1098	16.336	17.801	18.122	18.113
31	CVS3-31	998	9.757	10.502	10.705	10.726
37	CVS3-37	1449	53.487	58.628	59.281	59.497
37	CVS3-37	1350	41.917	46.333	47.239	47.275
37	CVS3-37	1251	31.266	34.424	35.326	35.384
37	CVS3-37	1150	21.968	24.116	24.896	24.983
38	CVS3-38	1449	54.246	58.375	59.777	59.469
38	CVS3-38	1350	41.521	46.599	47.321	47.150
38	CVS3-38	1250	31.166	34.887	35.604	35.572
38	CVS3-38	1150	22.204	24.513	25.257	25.255
39	CVS3-39	1448	42.350	49.297	48.888	48.859
39	CVS3-39	1350	34.345	36.203	37.027	37.067
39	CVS3-39	1250	25.829	27.697	28.271	28.333
39	CVS3-39	1150	18.296	19.883	20.326	20.418

#	Glass	T (°C)	EC 100	EC 1000	EC 10000	EC 100000
40	CVS3-40	1449	51.709	52.416	54.181	53.999
40	CVS3-40	1350	38.797	42.829	43.628	43.502
40	CVS3-40	1250	29.763	32.566	33.286	33.273
40	CVS3-40	1150	20.916	23.107	23.722	23.960

10.4 Crystallinity and Liquidus Temperature Results

CVS#	Glass	Quenched Glass Analysis			CCC Glass Analysis			TM	Liquidus	
		OM	SEM	XRD	OM	SEM	XRD		Tem	Pha
CVS3-1	Base line	No XL			3.7% XL inhomo	spinel		1366	1153	sp
CVS3-2	60 Si	No XL			very few spinel near crucible		Amourphous	1500	1181	sp
CVS3-3	45 Si	<<.1 undisolved cluster <<.1 spinel			2.2% XL spinel +?	spinel only		1213	1130	sp
CVS3-4	40 Si	2.6% spinel, possibly und Zr	spinel, (Si, Zr, Ce, Nd, [Na?])	5 vol% XL, 90w% sp, 10w% ZrCeO	13.2% XL 2 types	spinel, (Si,Ca,Nd, [Na?]), (Si, Zr, Ce, Nd, [Na?]), hiCr sp	35vol% XL, 45w%CaNdP O4SiO4, 35w%spinel, 20w%ZrCeO	1155	1186	Ce Zr Oy
CVS3-5	37 Si	3.6% spinel, possibly und. Zr	spinel	3 vol% XL, 75w% NiO, 25w% sp	33% XL 2 types (same as 3-4)	spinel, (Si,Ca,Nd, [Na?]), (Si, Zr, Ce, Nd, [Na?])	40vol% XL, 30w%CaNdP O4SiO4, 30w%spinel, 40w%ZrCeO	1165	1232	Nd Ce Zr Oy
CVS3-6	8 B	No XL			No XL			1237	1066	?
CVS3-7	4 B	No XL			No XL			1301	1132	sp
CVS3-8	22 Na	No XL			No XL			1182	1066	Na Zr Si
CVS3-9	5 Na	very small particles			4.4% XL spinel+?	spinel, hiCr sp		1529	1374	sp
CVS3-10	7 Li	No XL			<.1% stars (spinel?)	spinel, hiCr sp, hiNi sp		1153	1022 1021	Ce Sp
CVS3-11	5 Li	No XL			No XL			1257	1075	sp
CVS3-12	0 Li	very small particles	hi Cr spinel		Very high XL many phases,	spinel, hiCr sp		1557	1278	sp
CVS3-13	15 Fe	<.1% spinel	Spinel		5.9% tiny spinel at bottom, 4.5% larger spinel at top	spinel	10 vol% Spinel	1310	1295	sp
CVS3-14	11 Fe	No XL			sp 2.3%			1335	1227	sp
CVS3-15	0 Fe	No XL			no XL			1419	1111	Cr

CVS#	Glass	Quenched Glass Analysis			CCC Glass Analysis			TM	Liquidus	
		OM	SEM	XRD	OM	SEM	XRD		Tem	Pha
CVS3-16	25 Al	3.8% XL, inhomo	Spinel	10 vol% XL, 75w% sp, 25w% NdZrO	Fully XL? two distinct phases maybe more	(Si, Al), (Si, Al, Zr), (Si, Al, Zr, Nd, Fe), spinel	fully XL, 45w% LiAlSi, 40w% np, 10w% NaNdSi	1516	?	?
CVS3-17	18 Al	2.2% XL, inhomo			2.9% XL seem to be all spinel	spinel, (Si, Al, Nd [dend]), (Fe, Al, Ni [sp?])	25 vol% XL, 50w% NaNdSi, 35w% sp	1506	?	?
CVS3-18	13 Al	very small particles similar to 3-17			1.9% XL same as 3-17 only smaller			1457	1293	sp
CVS3-19	0 Al	No XL			No XL			1309	1070	sp
CVS3-20	16 Zr	3.1% XL inhomo, und Zr and other	ZrO2	10% ZrO2, YZrO type	6.7% XL	Zr, (Si, Fe, Zr, Ni)	15% ZrO2, Sp	1456	?	?
CVS3-21	12 Zr	.32% same as 3-20			3.6% XL more than one phase	Zr, spinel, hiCr spinel (spinel in Zr interstecies) streaks of Cr rich area	10 vol% XL, 60w% ZrO2, 40w% sp	1376	1400	Zr SiO 4
CVS3-22	8 Zr	No XL			1.6% XL same as 3-21			1366	1177	sp
CVS3-23	0 Zr	No XL			few tiny XL			1355	1122	sp
CVS3-24	20 Others	very small particles inhomo	Spinel	Amorphous	3.4% XL many phase inhomo	(Si, Ca, Nd, Ce), hiCr sp, spinel	5% Sp	1324	1127	sp
CVS3-25	7 Others	No XL			No XL			1411	1037 1050	hm sp
CVS3-27	15 Fe Dup cvs3-13	scattered spinel			Lots of colorful flowers and Botom agglom of XL	hiCr sp, spinel, (Nd, Si, Ca, Ce),	10vol% XL, 70wt% Spinel, 30wt% Ca5((Si,P,S)O 4)3F	1308	1285	sp
CVS3-28	4.4 Bi	No XL			<0.01 vol% sp	star shaped sp (Cr, Ni, Fe, Mn)	Amorphous	1349	1141	sp

CVS#	Glass	Quenched Glass Analysis			CCC Glass Analysis			TM	Liquidus	
		OM	SEM	XRD	OM	SEM	XRD		Tem	Pha
CVS3-29	6.4 Bi	No XL			<0.01 vol% sp	star shaped sp (Cr, Ni, Fe, Mn)	Amorphous	1336	1136	sp
CVS3-30	11.4 Bi	No XL			<0.01 vol% sp	star shaped sp (Cr, Ni, Fe, Mn)	Amorphous	1299	1121	sp
CVS3-31	16.4 Bi	No XL			few tiny XL	cube shaped sp (Cr, Ni	Amorphous	1261	1109	sp
CVS3-32	9.3 U			Amorphous			Amorphous	1388		
CVS3-33	3.3 U			Amorphous			Amorphous	1410		
CVS3-34	6.3 U			Amorphous			small amt of Al2O3, cp	1410		
CVS3-35	12.3 U			Amorphous			small amt of Ce2O3 and cp	1381		
CVS3-36	15.3 U			Amorphous			cp, CeO2 type crystals	1372		
CVS3-37	3 P	No XL		Amorphous	<0.01 vol%	sp (Cr, Ni, Fe, Mn)	2 vol% XL, Na3Nd(PO4)2, Li3PO4, NdPO4	1378	1175	sp
CVS3-38	5 P	No XL		1 vol% XL, NaNdPO4	0.21 vol%	Phase separated region of NaCaNdCeFe, sp, possible Li3PO4	8 vol% XL, Na3Nd(PO4)2, Li3PO4, NdPO4, sp	1391	1171	sp
CVS3-39	7 P	No XL		3 vol% XL, NaNdPO4	1.58 vol%	Phase separated region of NaCaNdLaCe FePNi, sp, possible Li3PO4	17 vol% XL, Na3Nd(PO4)2, Li3PO4, NdPO4, sp	1408	1168	sp
CVS3-40	9 P	No XL	phase separated	7 vol% XL, NaNdPO4	3.19 vol%	Phase separated region of NaNdCaPFe, sp, possible Li3PO4	22 vol% XL, Na3Nd(PO4)2, Li3PO4, NdPO4, sp	1417	1198	Zr Re Oy

10.5 PCT Normalized Releases for Each Glass

#	CVS	Si	B	Na	Li	pH	ccc Si	ccc B	ccc Na	ccc Li	ccc pH
1	CVS3-1	0.160	0.422	0.400	0.383	11.20	0.152	0.294	0.354	0.361	11.15
2	CVS3-2	0.132	4.803	0.306	0.360	10.80	0.131	0.262	0.286	0.328	10.77
3	CVS3-3	0.202	0.450	0.609	0.447	11.61	0.206	0.450	0.606	0.477	11.63
4	CVS3-4	0.254	0.654	0.907	0.595	11.88	0.359	0.430	1.381	0.908	11.88
5	CVS3-5	0.271	0.627	1.174	0.620	12.03	0.479	1.216	2.237	1.300	12.30
6	CVS3-6	0.151	0.309	0.296	0.346	10.23	0.144	0.273	0.265	0.302	10.17
7	CVS3-7	0.150	0.264	0.307	0.326	11.73	0.137	0.241	0.278	0.295	10.59
8	CVS3-8	0.585	1.266	2.625	1.643	12.45	0.580	1.548	2.462	1.477	12.42
9	CVS3-9	0.100	0.209	0.034	0.355	10.24	0.101	0.627	0.045	0.345	10.21
10	CVS3-10	0.334	0.703	0.824	0.865	11.85	0.319	0.000	0.732	1.324	11.79
11	CVS3-11	0.224	0.429	0.567	0.540	11.58	0.229	0.000	0.502	0.844	11.47
12	CVS3-12	0.113	0.100	0.314	0.000	10.79	0.114	0.268	0.299	0.000	10.64
13	CVS3-13	0.162	0.804	0.336	0.380	11.02	0.160	0.583	0.332	0.364	11.05
14	CVS3-14	0.155	0.301	0.346	0.356	11.06	0.200	0.503	0.614	0.554	11.51
15	CVS3-15	0.187	0.466	0.585	0.529	11.54	0.139	0.306	0.320	0.333	11.14
16	CVS3-16	0.120	0.268	0.079	0.511	10.35	0.117	1.250	0.037	0.418	9.46
17	CVS3-17	0.118	0.523	0.129	0.422	10.64	0.160	0.563	0.126	0.476	10.48
18	CVS3-18	0.111	0.643	0.199	0.304	10.74	0.112	0.302	0.199	0.301	10.70
19	CVS3-19	0.842	2.022	1.717	1.640	11.43	0.743	2.220	1.470	1.398	11.30
20	CVS3-20	0.110	0.181	0.298	0.331	11.03	0.135	0.804	0.364	0.396	11.18
21	CVS3-21	0.097	0.196	0.254	0.301	11.03	0.124	0.530	0.322	0.359	11.14
22	CVS3-22	0.119	0.324	0.303	0.310	11.07	0.118	0.432	0.303	0.330	10.97
23	CVS3-23	0.232	0.402	0.562	0.502	11.28	0.228	0.515	0.528	0.481	11.17
24	CVS3-24	0.151	0.261	0.380	0.355	11.07	0.155	0.362	0.342	0.356	10.97
25	CVS3-25	0.161	0.209	0.420	0.384	11.26	0.156	0.338	0.382	0.368	11.18
26	CVS3-27	0.157	0.342	0.329	0.358	10.98	0.159	0.704	0.391	0.395	11.15
27	CVS3-28	0.160	0.305	0.400	0.382	11.21	0.157	1.094	0.366	0.365	11.09
28	CVS3-29	0.189	0.241	0.432	0.411	11.22	0.155	0.531	0.381	0.376	11.16
29	CVS3-30	0.183	0.338	0.420	0.397	11.23	0.159	0.463	0.379	0.385	11.03
30	CVS3-31	0.202	0.261	0.465	0.451	11.25	0.156	2.311	0.376	0.382	11.05
31	CVS3-32	0.159	0.487	0.326	0.370	10.88	0.155	0.412	0.289	0.367	10.84
32	CVS3-33	0.149	0.403	0.335	0.338	10.95	0.144	0.368	0.299	0.334	10.87
33	CVS3-34	0.154	0.411	0.331	0.357	10.89	0.151	0.394	0.297	0.369	10.88
34	CVS3-35	0.163	0.422	0.325	0.395	10.78	1.740	0.441	0.343	0.468	10.94
35	CVS3-36	0.165	0.543	0.304	0.393	10.80	0.174	0.523	0.313	0.458	10.88
36	CVS3-37	0.151	0.547	0.370	0.188	10.52	0.152	0.294	0.361	0.354	10.96
37	CVS3-38	0.147	0.418	0.327	0.292	11.03	0.120	0.370	0.283	0.326	10.90
38	CVS3-39	0.121	0.209	0.252	0.234	10.81	0.130	0.242	0.286	0.681	10.89
39	CVS3-40	0.141	0.225	0.248	0.205	10.59	0.168	0.290	0.359	1.055	10.72